Botanical Journal of the Linnean Society, 2021, **195**, 650–670. With 8 figures.

Novelties in the secretory structures of three species of *Gongora* (Orchidaceae: Stanhopeinae)

JORGEANE V. CASIQUE[1]*, ELOISA H. DE AGUIAR ANDRADE[2], ANA CRISTINA ANDRADE DE AGUIAR DIAS[3] and ALEXANDRA A. MASTROBERTI[1]

[1]*Programa de Pós-graduação em Botânica, Departamento de Botânica, Universidade Federal do Rio Grande do Sul, Porto Alegre, RS 91501–970, Brazil*
[2]*Programa de Pós-Graduação em Biodiversidade (Bionorte), Departamento de Botânica, Museu Paraense Emílio Goeldi, Belém, PA 66077–830, Brazil*
[3]*Instituto de Ciências Biológicas, Universidade Federal do Pará, Belém, PA 66075–110, Brazil*

Received 8 January 2020; revised 2 June 2020; accepted for publication 9 July 2020

The members of the Stanhopeinae (Orchidaceae) bear osmophores, which are related to pollination since they exude volatile lipids that attract euglossine bees. *Gongora* spp. are pollinated exclusively by euglossine bees. In view of the structural diversity found in the flowers of this genus and the lack of data on other foraging insects that visit these flowers, we elucidated aspects of the anatomy of floral secreting structures in the Stanhopeinae group, focusing on structures in *Gongora jauariensis*, *Gongora pleiochroma* and *Gongora minax*, species from the Amazon Rainforest. Secretory structures were analysed using light, scanning and transmission electron microscopy, and histochemical and phytochemical procedures. Osmophores, extrafloral nectaries and elaiophores were observed. The three species bear a structured nectary on the bract and osmophores on both the sepals and labellum hypochile. In *G. minax*, the labellum (hypochile) shows chemical and structural characteristics of elaiophore and osmophores, suggesting that it has both functions. We report interactions between foraging ants and nectaries of *Gongora* spp. for the first time. Interactions with ants attracted by the nectaries on the bracts are beneficial for orchids, as the ants help to protect their reproductive structures.

ADDITIONAL KEYWORDS: Amazon – anatomy – floral fragrance – histochemistry – nectaries.

INTRODUCTION

Osmophores, elaiophores and nectaries are found in members of the Orchidaceae and are important elements for maintaining the plant-pollinator interaction (Melo, Borba & Paiva, 2010; Aguiar *et al.*, 2012; Pansarin *et al.*, 2012; Nunes *et al.*, 2013; Neubig *et al.*, 2015; Franken, Pansarin & Pansarin, 2016; Kettler, Solís & Ferrucci, 2019). However, in flowers of species of the subtribe Stanhopeinae (Cymbidieae: Epidendroideae), only osmophores located on the adaxial surface of the sepals, petals or labellum have been reported (Curry *et al.*, 1991; Pansarin, Castro & Sazima, 2009; Pansarin & Pansarin, 2011; Antón, Kamińska & Stpiczyńska, 2012; Davies & Stpiczyńska, 2012; Francisco & Ascensão, 2013; Adachi, Machado & Guimarães, 2015; Davies & Stpiczyńska, 2017; Casique *et al.*, 2018). These osmophores are comprised of papillose or non-papillose epidermal secretory cells, characterized as unicellular secretory trichomes (Curry *et al.*, 1991; Stpiczyńska, 1993; Ascensão *et al.*, 2005; Melo *et al.*, 2010).

The Stanhopeinae are a monophyletic Neotropical subtribe, with *c*. 304 species in 20 genera (Dressler, 1993; Chase *et al.*, 2003; Pridgeon *et al.*, 2009; Chase *et al.*, 2015). Approximately 37 species of Stanhopeinae occur in the Brazilian Amazon (Flora do Brasil, 2020). Species of this subtribe are epiphytic or terrestrial herbs, with uninodal pseudobulbs, articulate, often petiolate terminal leaves and lateral inflorescences (Rasmussen, 1985; Dressler, 1993; Whitten, Williams & Chase, 2000).

The flowers have high morphological plasticity and are among the most fascinating and curious orchids, due to their ingenious mechanisms for pollination, which is performed exclusively by male euglossine bees

*Corresponding author. E-mail: valerytvares@hotmail.com

(Dressler, 1993; Gerlach, 2003; Gerlach & Dressler, 2003). The high complexity of flowers in the Stanhopeinae has encouraged recent studies that focused primarily on the structure of the labellum, which is divided into three regions: hypochile (basal), mesochile and epichile (apical) (Gerlach, 2003, 2011; Antón *et al.*, 2012; Adachi *et al.*, 2015; Nunes *et al.*, 2017).

Recent studies on secretory structures of *Stanhopea grandiflora* (Lodd.) Lindl. have also found nectaries on the bract and colleters on the ovary surface (Casique *et al.*, 2018). The mucilage in this ovary region in species of Pleurothallidinae functions to protect microorganisms and herbivores and to enable symbioses with fungi that are necessary for seed germination (Cardoso-Gustavson *et al.*, 2014).

Gongora Ruiz & Pav. is one of the most taxonomically complex genera of Stanhopeinae, due to the high morphological variability of certain species, particularly concerning flowers, colours and scents (Rudolf, 1993). In *Gongora,* the mesochile (labellum) is inverted, and bees forage hanging upside down, sliding backward to the column apex below and moving the pollinarium (Whitten *et al.*, 2000; Adachi *et al.*, 2015).

In recent studies on pollination ecology, floral scent and morphology were used to elucidate pollination mechanisms in *Gongora* (Adachi *et al.*, 2015). Osmophores are papillose and found in the labellum area, referred to as the hypochile (Adachi *et al.*, 2015; Nunes *et al.*, 2017). The fragrance synthesized in the osmophores attracts male euglossine bees as a reward (Curry, 1991). These volatile compounds are actively exploited by species of Euglossini (Apidae) and stored in the posterior tibia, a specialized structure of these bees (Adachi *et al.*, 2015; Nunes *et al.*, 2017; Casique *et al.*, 2018). Although the precise function of these fragrances in bee biology has not been elucidated, some investigators believe that the fragrances might be used as precursors for synthesis of a sex pheromone (Dressler, 1982; Bembé, 2004). Certainly, fragrance production is a key element in the evolution of many orchids (Nunes *et al.*, 2017).

Of the 11 *Gongora* spp. occurring in Brazil, eight have been reported in the Brazilian Amazon (Flora do Brasil, 2020). Despite their wide occurrence in this region, studies involving the ecological relationships of male bees of the Euglossini and other floral visitors to their flowers are sparse, which hampers understanding, not only of the secretion processes and the floral reward they can offer, but also of insect-plant interactions in these species.

Following a study of *S. grandiflora*, which addressed pollination ecology, floral aroma and floral morphology, and especially conducted anatomical analyses of its secretory structures and their relationships to floral visitors (Casique *et al.*, 2018), we here investigate *Gongora* spp. to analyse other secretory structures that might be present in this genus and how they contribute to the adaptive success of these species.

We investigated anatomical, histochemical and phytochemical aspects of the floral and extrafloral glands of three *Gongora* spp. We also identified and characterized these structures to aid in understanding their secretion dynamics and their ecological relationships to floral and extrafloral visitors.

MATERIAL AND METHODS

Plant material and field observation

Flowers in preanthesis and anthesis stages were collected from the same inflorescence of eight individuals of three species of *Gongora*: *G. pleiochroma* Rchb.f., *G. jauariensis* Campacci & J.B.F.Silva and *G. minax* Rchb.f., in January and February, in the morning (06:00-07:00). Sampling was conducted in the state of Pará, Brazil, at the following localities: Ananindeua, Belém, vicinity of the Jari River, Santarém, Santo Antônio do Tauá, Santa Izabel and Oriximiná. These species are epiphytes and occur near rivers and streams. The first flowers and floral visitors were recorded using photographs and videos where they were observed. Bees observed on *G. minax* took some time (*c.* 15 min) to approach the flowers; this delay lasted only 5 min in *G. pleiochroma* and *G. jauariensis*.

The terminology adopted by Remizawa *et al.* (2013) is used to classify the inflorescences as flower-subtending bracts, here termed bracts. After flowering, the flowers were labelled and fertile plants were removed to make exsiccates, which were incorporated into the collections of the João Murça Pires Herbarium at the Museu Paraense Emílio Goeldi (MG) and the Herbarium of the Universidade Federal do Rio Grande do Sul (ICN); voucher numbers are *MG150592* for *G. pleiochroma*, *MG221264* for *G. minax* and *ICN 199992* for *G. jauariensis*.

Sampled specimens were subsequently cultivated in a private orchidarium under abiotic conditions similar to the natural environment for observation of subsequent flowering events and potential floral visitors. Only bracts were analysed in the preanthetic stage; the other analyses were performed during anthesis. Flowers in preanthesis and anthesis were isolated with a screen for *c.* 1 h to protect them from visitors. Although nectar production was detected in the bracts, the volumes produced were insufficient to measure. Glucose test strips were used (Glicofita Plus®, Accu-Chek Active, F. Hoffmann-La Roche Ltd.) to check the occurrence of glucose in the glandular secretions.

The orchid species were identified by Mr. João Batista Fernandes da Silva, an expert on Amazonian orchids. Foragers observed were collected and conserved in commercial ethanol; these were identified by Dr. Fernando Carvalho, an entomologist from the Museu Paraense Emílio Goeldi.

Light microscopy

For anatomical analyses, flowers (labellum, sepals) and bracts were collected and fixed in 1% glutaraldehyde, 4% formaldehyde and 0.1 M sodium phosphate buffer, pH 7.2 (McDowell & Trump, 1976), dehydrated in an ascending ethanol series (10%, 30%, 50%, 70%, 90% and 100%), and embedded in hydroxyethyl methacrylate [Leica® historesin (Gerrits & Smid, 1983)]. Serial cross-sections and longitudinal sections *c*. 3 µm thick were made using a rotary microtome (Leica Autocut) and stained with toluidine blue O (C.I. 52040), pH 4.4 (O'Brien, Feder & McCully, 1964). Permanent slides were mounted in Canada balsam and observed by light microscopy in bright field (Leica DMR).

Histochemical tests

Fresh material of labella, sepals and bracts was used for the following histochemical tests: Lugol's reagent for starch detection (Johansen, 1940), Fehling's reagent for reducing sugars (Sass, 1951), Sudan III for lipids (Johansen, 1940), Sudan IV for lipids (Pearse, 1980), neutral red under fluorescence for lipids (Kirk-Junior, 1970), Nile blue sulphate for neutral and acid lipids (Cain, 1947), copper acetate and rubeanic acid for fatty acids (Ganter & Jollès, 1969, 1970), NADI reagent for essential oils and resins (David & Carde, 1964) and xylidine Ponceau for total proteins (Vidal, 1970). Untreated samples were also analysed, and negative control tests were carried out. Negative controls were performed in the test for lipids (Sudan III, Sudan IV, NADI reagent, Nile blue sulphate, copper acetate and rubeanic acid), for which sections were washed with a solution of methanol/chloroform/H_2O/HCl (66: 33: 4: 1) for 1 h at room temperature before the test was performed. Analyses were conducted and photomicrographs taken under light microscopy in bright field (Leica DMR), except for neutral red, which was observed under epifluorescence in UV light (excitation filter 450–490 nm). Images were acquired with a digital camera (AxioCam HRc, Zeiss) coupled to the microscope. The program ZEN Light 2012 was used for image capture. Structural nomenclature is based on Metcalfe & Chalk (1950), Withner, Nelson & Wejks-Nora (1974), Fahn (1979), Vogel (1990) and Curry *et al.* (1991).

Chemical analyses

The labella of fresh flowers (anthesis) were submitted to extraction (3 h) in a simultaneous distillation-extraction microsystem to obtain the volatile concentrates, using a Likens & Nickerson-type apparatus (Likens & Nickerson, 1964) and pentane as the solvent (4 mL). Volatile concentrates were analysed by GC-MS, using a QP-2010-Plus gas chromatograph mass spectrometer (Shimadzu Corporation, Tokyo, Japan) and a silica capillary column (Rtx-5ms, 30 mm × 0.25 mm × 0.25 µm film thickness), with the aid of MS Solution software and standard libraries (Jennings & Shibamoto, 1980; Adam, 2007; Mondello, 2011). The analysis conditions were: injector temperature 250 °C; oven temperature programming 60–250 °C (3 °C/min); helium carrier gas (32 cm/s) measured at 100 °C; splitless-type injection of 1.0 µL of the sample; ionization by electron impact, 70 EV; and temperatures of ion source and transfer line 220 °C and 250 °C, respectively. Mass spectra were obtained by automatic scanning (0.3 s each), with mass fragments varying from 40 to 450 m/z. The retention index was calculated for all volatile components, using a homologous series of alkanes (C_8–C_{20}, Sigma-Aldrich) according to Van Den Dool & Kratz (1963). Constituents were identified by comparing their retention indices and mass-spectra libraries (molecular mass and fragmentation pattern), as well as consulting the mass-spectra literature. The analysis was undertaken at the Adolpho Ducke Laboratory of the Museu Paraense Emílio Goeldi.

Scanning electron microscopy

For scanning electron microscopy (SEM), the fixed material (bract, sepals and labella) was dehydrated in a graded acetone series and critical-point dried (Gersterberger & Leins, 1978) with a CPD 030 Balzers dryer. The material was attached to aluminium stubs with double-sided carbon tape, metallized with gold in a BAL-TEC SCD 050 (Balzers) sputter coater and analysed using a JEOL 6060 SEM at the Microanalyses and Microscopy Center (CMM) of the Universidade Federal do Rio Grande do Sul (UFRGS).

Transmission electron microscopy

Labella of each species were fixed in 2.5% glutaraldehyde, 2.0% formaldehyde in 0.1 M sodium phosphate buffer, pH 7.2, and post-fixed in 1% osmium tetroxide in 0.1 M sodium phosphate buffer, pH 7.2. The samples were then washed in the same buffer (two changes of 30 min/stage) and distilled water (two changes of 30 min/stage). The material was dehydrated in an acetone series (10%, 30%, 50%, 70%, 90% and 100%) for 30 min in each stage and finally for 15 min in acetonitrile. The material was

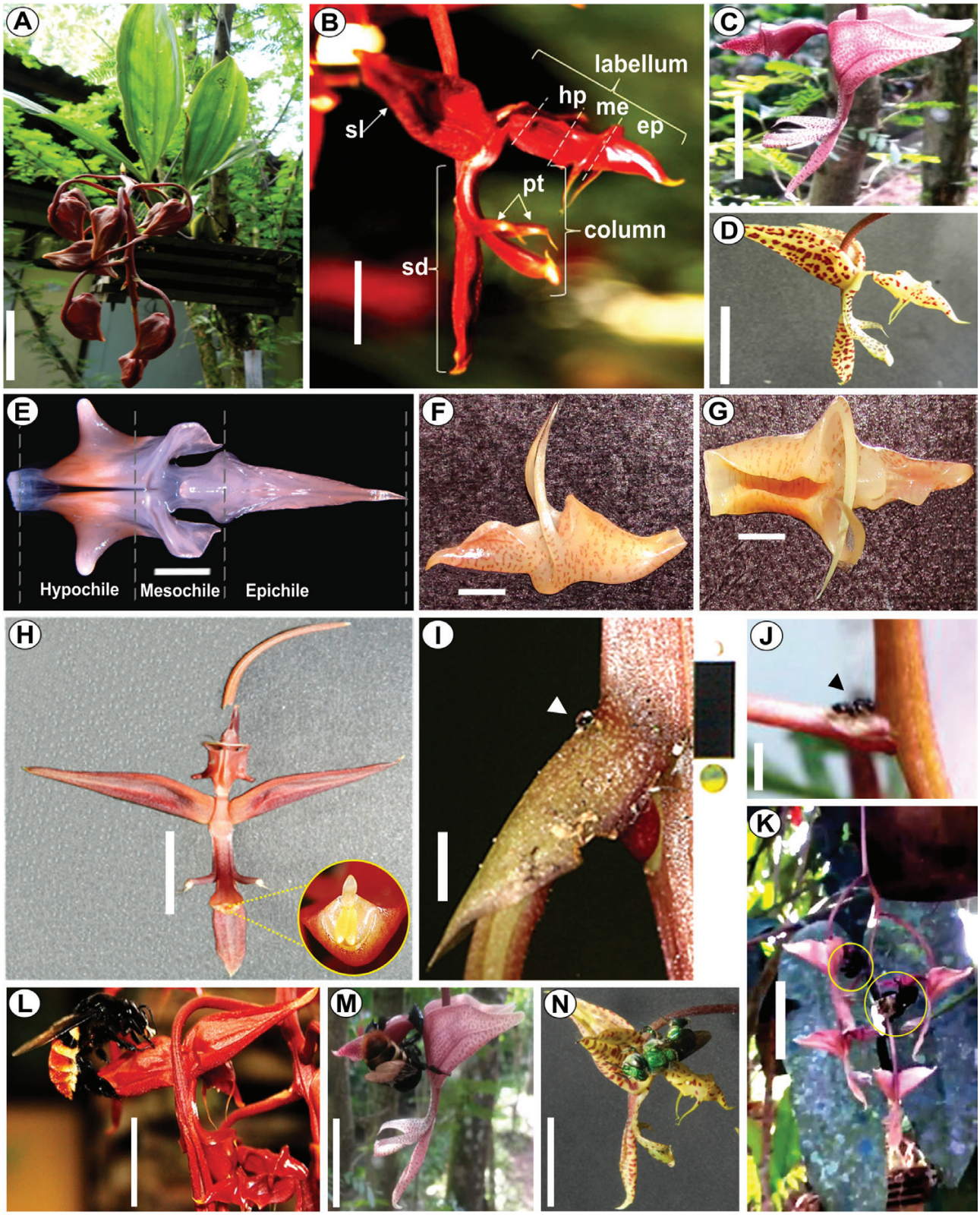

Figure 1. Habit and morphology of *Gongora*. A, habit and pendant inflorescence. B, postanthesis flower of *G. jauariensis*. C, flower of *G. minax*. D–E, flower of *G. pleiochroma*. F–G, morphology of *G. minax*, frontal and lateral view; note the absence

first embedded in a pure acetonitrile solution (0.5 mL) and dipped every 10 min in a low-viscosity epoxy resin (Spurr, 1969) until a 1:1 ratio was achieved, for 12 h. The material was transferred to a solution of resin/acetonitrile at a 3:1 ratio and was subsequently embedded in pure resin, remaining for 12 h in each stage. Embedding and polymerization were carried out in jelly capsules, with the material placed in an incubator at 70 °C for 18 h.

These blocks were sectioned to approximately 70 nm thick, using an ultramicrotome (Leica Ultracut UCT) and a diamond blade. These ultrathin sections were placed on copper grids of mesh size 200 and stained using 2% uranyl acetate in aqueous solution and lead citrate (modified from Hanaichi *et al.*, 1986).

Transmission electron microscopy (TEM) images were obtained at CMM, Universidade Federal do Rio Grande do Sul using a JEOL JEM 1200 EX II.

RESULTS

Morphological aspects

The genus Gongora

The inflorescence is a pendant raceme and rises at the base of the pseudobulb, bearing ten to 20 flowers with flower-subtending bracts (Fig. 1A). Flowers are non-resupinate, often scented; the colour varies, especially between brown and yellow tones. The flowers are sometimes smooth and sometimes have maculae (Fig. 1B–D). Sepals are free from each other and feature a revolute margin. The dorsal sepal is erect and the lateral sepal is patent on the labellum or reflex; the petals are patent, smaller than the sepals. The labellum is ornamented with horns (a diagnostic feature for the genus) and is divided into three segments: the hypochile, frequently with horns; the mesochile always with bristles; and the epichile with a bulge and a triangular extremity (Fig. 1E–H). The column is long, narrow and slightly curved (Fig. 1H). The two pollinia are yellow and connected to a shield-shaped stipe (Fig. 1H). The viscidium is triangular or rounded. *Gongora* is subdivided into three subgenera: *Acropera* (Pfitzer) Jenny, *Gongora* and *Portentosa* Jenny. The above characteristics correspond to *Gongora* subgenus *Gongora*, to which the species analysed in this study belong.

The species exhibit some similar morphological characteristics. For example, the flowers of *G. jauariensis* (Fig. 1B) and *G. pleiochroma* (Fig. 1D) are c. 2–3 cm long (Fig. 1H) whereas those of *G. minax* are c. 4–5 cm long (Fig. 1C).

Ecological interactions

Ants (*Dolichoderus* sp.) were observed foraging in the basal region of the flower bract in the preanthetic and anthetic stages (Fig. 1I, J). An analysis of the secretion with glucose test strips (> 25.0 mmol/L) in this region was positive for all three species (Fig. 1I). During anthesis, which occurred between 06:00 and 07:00, the presence of male euglossine bees (*Eulaema bombiformis* and *Euglossa* sp.) differed with regard to their preferences for scent (Fig. 1K–N) on the sepals and labella (Fig. 2A–C). In *G. pleiochroma* and *G. jauariensis*, both with a strong minty scent, only bees of *Euglossa* sp. were observed foraging on the flowers, whereas both *Eulaema bombiformis* and *Euglossa* sp. were present on the labella and sepals of *G. jauariensis* and *G. minax* (Fig. 2C–D). The scent of *G. minax* was similar to that of the other species, although less pungent and perceptible to human beings. The bee *Eulaema nigrita* was observed foraging on the labellum (hypochile) of *G. minax* together with male *Eulaema bombiformis* (Fig. 1K, L). It was not possible to collect a specimen of *Eulaema nigrita*, which was identified from video recordings.

The pollination mechanism was similar in all species: bees landed specifically on the labellum (mesochile) and foraged in the adaxial and abaxial regions, where the osmophores are situated. When bees were placed upside down to explore the ventral region of the labellum (hypochile), they showed a slight imbalance and touched the column apex (gynostemium) where the viscidium is located. The viscidium has a glue-like substance that develops at the tip of the stigma, and when the bee touches it, the viscidium projects the pollinarium into the scutellum of the pollinator (Fig. 2C).

of horns in the labellum. H, frontal view of flower of *G. pleiochroma*, detail of pollinarium. I–J, bract tested with Glicofita Plus (arrows) and foraging ants (*Dolichoderus* sp.) (arrows). K, *Eulaema nigrita* (smaller circle) and *Eulaema bombiformis* (larger circle) on the labellum of *G. minax*. L, detail of *Eulaema bombiformis* on the sepals of *G. jauariensis*. M, *Euglossa* sp. on the sepals of *G. pleiochroma*. N, *Eulaema bombiformis* on the labellum of *G. minax*. Scale bars: A, C, I = 2 cm; B, D, H, N = 1 cm; E, J = 1 mm; F, G, L, K = 5 mm; M = 5 cm. Key to all figures: sl, lateral sepals; sd, dorsal sepals; pt, petals; co, column; hp, hypochile; me, mesochile; ep, epichile; cu, cuticle; cw, cell wall; is, intercellular space; mi, mitochondria; nu, nucleus; se, lipid secretion; sg, starch grains; pl, plasmalemma; va, vacuole; ve, vesicles.

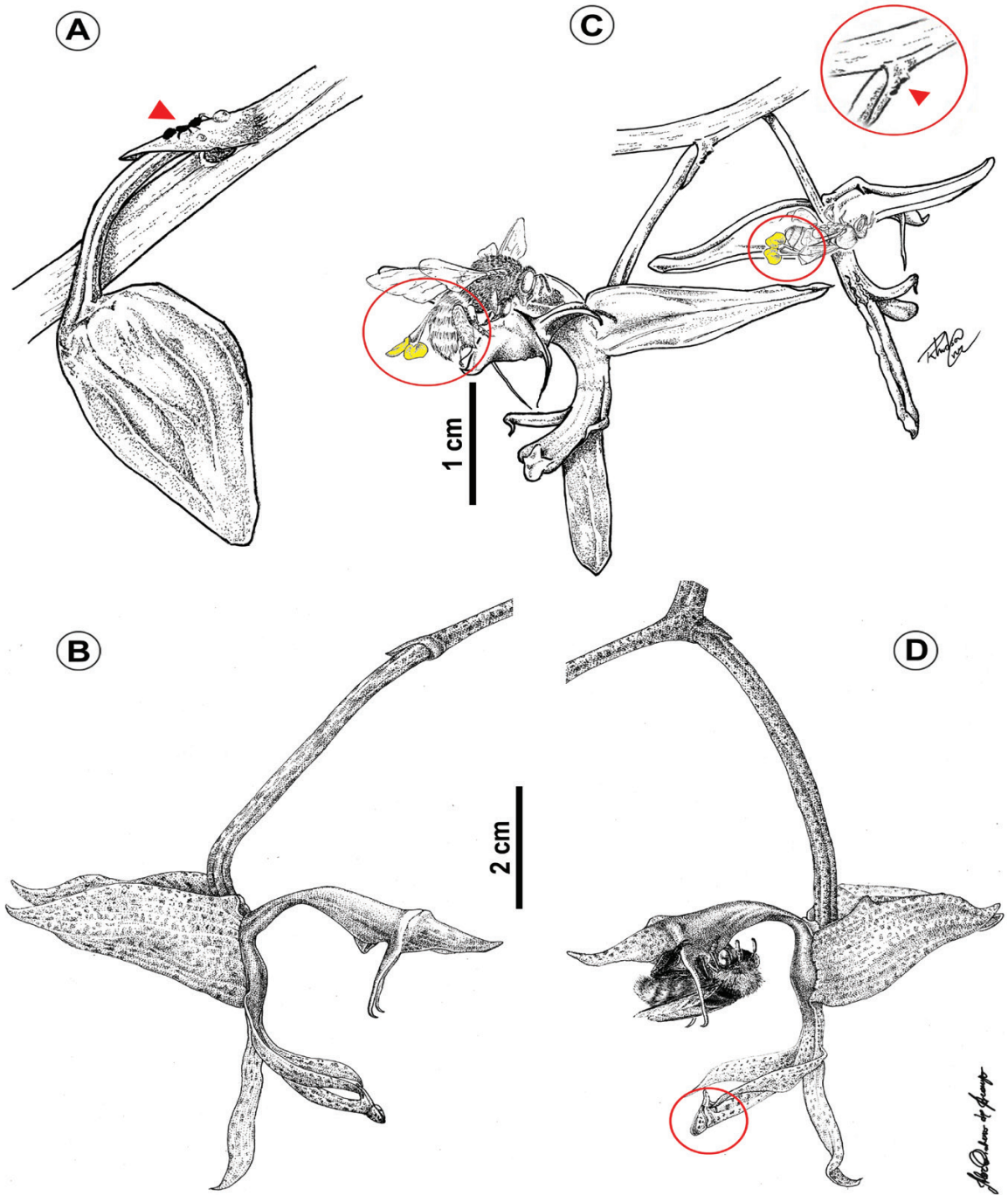

Figure 2. Foragers, pollinators and pollination mechanism in *Gongora*. A, floral bud of *G. pleiochroma* with *Dolichoderus* sp. ant on bract (red arrow). B, flower of *G. minax* at anthesis. C, scheme of flowers of *G. jauariensis* (left) with *Eulaema bombiformis* (red circle) foraging the labellum and *G. pleiochroma* (right) with *Euglossa* sp. (red circle) foraging the sepal; note the pollinarium (highlighted in yellow) on the scutellum of the bee; the detail (red circle) shows the ant foraging the bract of post-anthetic flowers. D, bee (*Eulaema nigrita*) on the labellum of *G. minax*, entering the excavated hypochile in search for oleiferous compounds collected from the base of the hypochile; detail of column apex with pollinarium (red circle); after the bee forages the labellum, it falls on the column, and the pollinarium clings to the scutellum. Scale bars: A, C = 1 cm; B, D = 2 cm.

Anatomy of bracts, labella and sepals

Bracts

The nectaries are present only on the base of the bract (Fig. 3A), on the epidermis of the abaxial surface (Fig. 3B) and comprised of cells with a thick cuticle. The secretory gland on the abaxial surface of the bract in *G. jauariensis*, *G. minax* and *G. pleiochroma* has an epidermis with the outer periclinal walls convex to papillose and the inner periclinal walls convex to straight; the mesophyll has one to three layers of nectary parenchyma, followed by one to five layers of ground parenchyma with anisodiametric thin-walled cells (Fig. 3A, B), raphide crystal idioblasts (Fig. 3C, D) and collateral vascular bundles enclosed by a sclerenchymatic sheath (Fig. 3E). Stomata (Fig. 3F, G) and digitiform trichomes were observed on the adaxial (cross-section and frontal views) and abaxial surfaces of the bract (Fig. 3H–J).

Sepals

The epidermal osmophore is located in the epidermis of the adaxial surface of sepals of all three species, visible in cross-section and frontal view. The epidermal cells (abaxial surface) of sepals in *G. jauariensis* (Fig. 4A) and *G. pleiochroma* (Fig. 4B) have outer periclinal walls slightly thick and convex (Fig. 4C–E); the cells of osmophores on the adaxial surface are papillose, conical and have lateral ridges, elongated

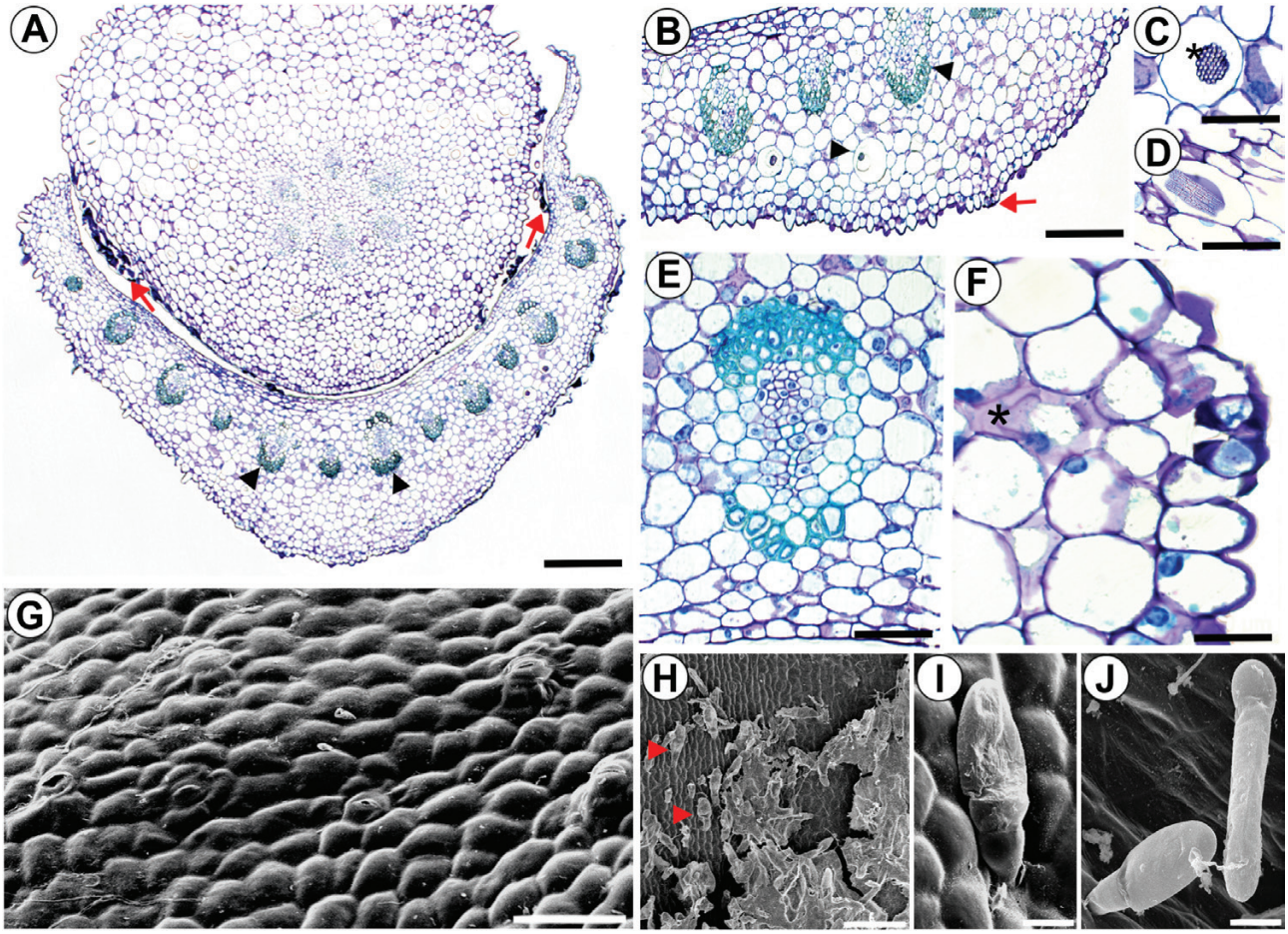

Figure 3. Structural analysis of bract by light microscopy (A-F) and SEM (G–J) in *Gongora* species. A, B, I, *G. jauariensis*. C, D, G, H, *G. pleiochroma*. E, F, J, *G. minax*. A, cross-section of the bract adnate to pedicel, collateral vascular bundles ordered in mesophyll (arrow head), digitiform trichomes in the adaxial surface (arrows). B, crystalliferous idioblasts in bract mesophyll and vascular bundle (arrow head), stomata on the abaxial surface (arrows). C–D, detail of bract idioblasts with raphides. *, highlight for a detail. In case, the raphides. E, collateral vascular bundles of the bract. F, nectaries on the abaxial surface of bract, with content visible in intercellular spaces (*). G, in SEM, stomata observed on the abaxial surface of bract of *G. pleiochroma*. H, digitiform trichomes along the adaxial surface of bract (arrowhead). I–J, detail of this digitiform trichomes observed on the abaxial surface of bract. Scale bars: A = 200 µm; B = 100 µm; C–E = 20 µm; F = 10 µm; G, H, J = 20 µm; I = 10 µm.

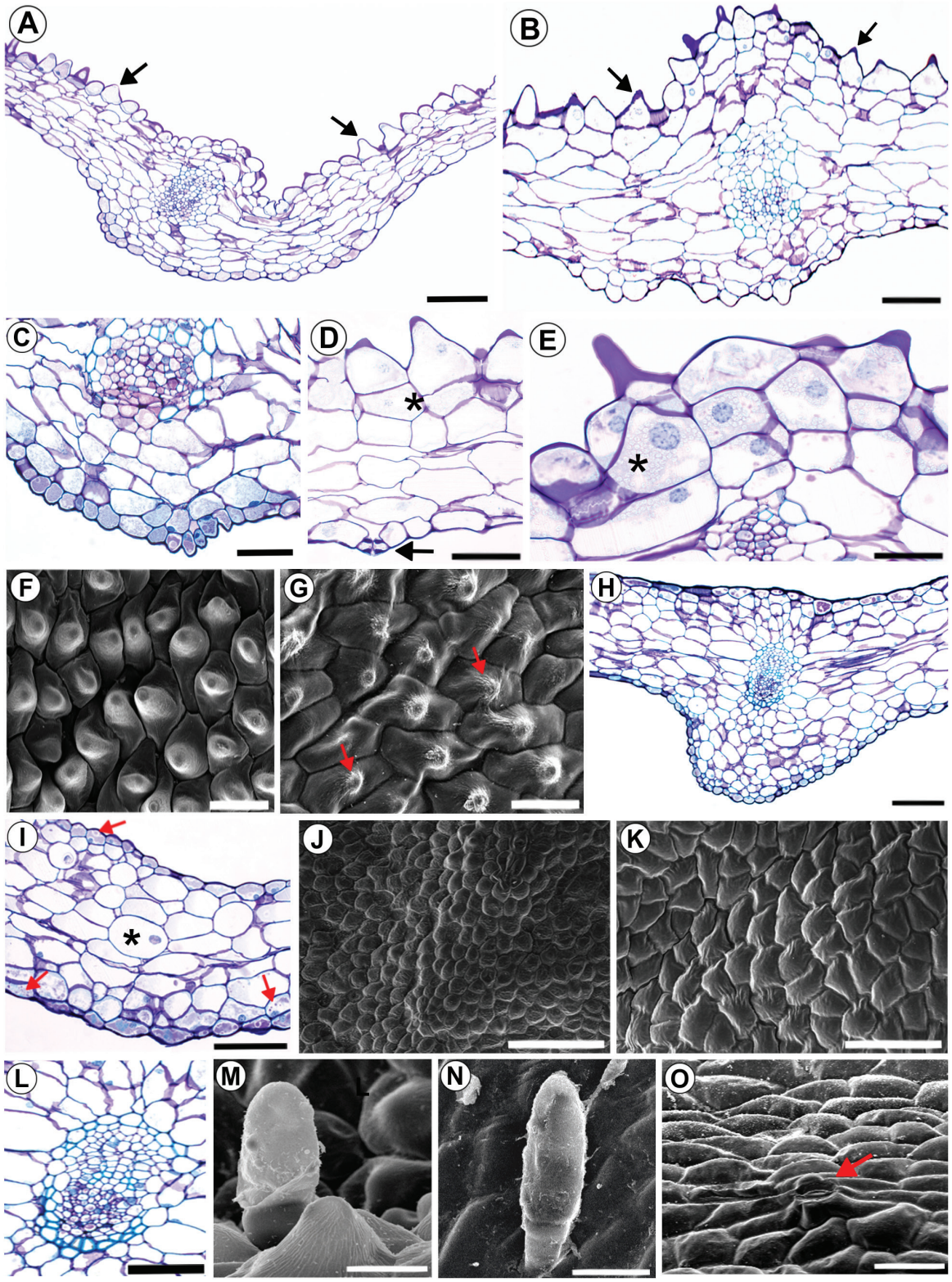

Figure 4. Osmophore in the sepal of *Gongora* species. A–E, H–I light microscopy; F, G, J, K SEM. A, *G. jauariensis*, papillose cells of secretory epidermis (arrows). B, papillose cells (arrows) of secretory epidermis in the sepal of *G. pleiochroma*. C, collateral vascular bundle in the mesophyll close to abaxial surface. D, adaxial surface of sepal, with starch grains in the detail (*) of papillose cells, stomata on the abaxial surface (arrows). E, adaxial surface of sepal showing starch grains in the

in *G. pleiochroma* (Fig. 4F) and short in *G. jauariensis* (Fig. 4G); the sepals of *G. jauariensis* have epicuticular wax (Fig. 4G). In *G. minax* (Fig. 4H, I) the cells of osmophores on the adaxial surface are convex and straight. In all three species, the outer periclinal walls are thick; the inner periclinal walls are thin, slightly sinuous to curved; the anticlinal walls are slightly sinuous; the epidermal cells on the abaxial surface of sepals are elongate, with the outer and inner periclinal walls slightly curved and the anticlinal walls straight; and, in frontal view, the cells are polygonal (Fig. 4J, K); the mesophyll is comprised of multiseriate parenchyma cells, large, sinuous, and thin-walled, with sparse collateral vascular bundles (Fig. 4L), abundant starch (Fig. 4D, E) and idioblasts with calcium oxalate crystals (Fig. 4I). Digitiform trichomes were rarely observed, and only on the adaxial surface of the sepals (Fig. 4M, N); stomata were only observed on the abaxial surface of the sepals (Fig.4D, O). A thin layer of epicuticular wax is visible on the abaxial surface of sepals in *G. minax*, in frontal view (Fig. 4O).

Labella

The osmophores on the labellum (hypochile) in *G. jauariensis* (Fig. 5A–E) and *G. pleiochroma* (Fig. 5F–J), in cross-section and frontal views, have the papillose epidermis of the ventral surface and the non-papillary epidermis of the dorsal surface as the main secretory tissues. The cells of the labellum contain a large nucleus and dense cytoplasm. The parenchyma below the secretory tissue is adjacent to the epidermis, with vacuolated cells (Fig. 5C, I); the dorsal surface is also comprised of papillose and secretory cells; the subjacent parenchyma is comprised of anisodiametric cells, thin and with dispersed collateral vascular bundles. In *G. minax* (Fig. 5K–O), the osmophores are also present in the labellum (hypochile). Unlike the other two species, in *G. minax* the labellum area (hypochile) on the ventral and dorsal surface of labellum has a double function, as an osmophore and an elaiophore. The secretory epidermis (ventral surface) of this area is palisade with cuboid to ovoid cells (cross-section) with a large nucleus, thick wall, dense cytoplasm, lipid drops (Fig. 5M), stomata and epicuticular wax (Fig. 5O); it is followed by six parenchyma layers with vacuolated cells and evident intercellular spaces (Fig. 5I); the epidermis of the dorsal surface (Fig. 5L) is also secretory and has cell characteristics similar to those on the ventral surface, with stomata absent (Fig. 5L); the ground parenchyma consists of anisodiametric cells, thin, vacuolated, with intercellular spaces and collateral vascular bundles (Fig. 5D, I, K).

Histochemistry

For all three species, the histochemical analysis of the bract nectaries revealed the presence of monosaccharides or reducing sugars (Fig. 6A–D), total proteins (Fig. 6E–G) and starch (Fig. 6H). The osmophores of the sepals contained lipids (Fig. 6I–K) and terpenoids (Fig. 6L, M). In the region of the labellum – osmophore (hypochile), the tests indicated total lipids (Fig. 7A–E), starch (Fig. 7F–H), terpenoids – essential oils (Fig. 7I–K) and terpenoids – resin acids (Fig. 7L), and acid and neutral lipids (Fig. 7M–N). The analysis also revealed fatty acids in the elaiophore of *G. minax* (Fig. 7O) and total lipids under UV light in *G. pleiochroma*, *G. jauariensis* (Fig. 7P) and *G. minax* (Fig. 7Q).

Transmission electron microscopy

Osmophores and elaiophores

Epidermal cells in the ventral and dorsal regions of the labellum (hypochile) were analysed. Papillose cells of the secretory epidermis of osmophores in *G. jauariensis* and *G. pleiochroma* have similar features (Fig. 8A–E), i.e. dense cytoplasm with lipid drops, vesicles and a vacuole with polysaccharide content (Fig. 8A). The cuticle layer shows an electron-dense microchannel net (Fig. 8B). Other papillose cells have a voluminous nucleus, dense nucleolus, dense cytoplasm with developing vacuoles and intercellular spaces (Fig. 8A). The parenchyma cells have well-developed vacuoles (Fig. 8C). Mitochondria and smooth and rough endoplasmic reticulum (Fig. 8D) were found near the periplasmic space (Fig. 8C). Vesicles and abundant amyloplasts associated with plastoglobuli were observed in the cytoplasm (Fig. 8C, E), as were drops of lipid.

In *G. minax* the thick cuticle also exhibited a well-developed net of microchannels and deposits of epicuticular wax (Fig. 8F–H). The outer periclinal wall is polylamellate and has microchannels.

parenchyma cells (*). F, elongated ridges in *G. pleiochroma* sepals. G, short ridges in *G. jauariensis*, in the detail epicuticular wax (arrows). H, smooth osmophore in the sepal of *G. minax*. I, crystalliferous idioblasts along the mesophyll, evident lipid drops (arrows). *, highlight for a detail. In case, the starch grains. J, abaxial surface of sepals of *G. pleiochroma*. K, abaxial surface of *G. minax* sepal. L, detail of collateral vascular bundle in the sepal of *G. minax*. M–N, digitiform trichomes observed on the adaxial surface of sepals of *G. jauariensis*. O, stomata present on the abaxial surface of *G. minax* sepals. (arrows) Scale bars: A–C = 500 µm; D, E, I, L = 100 µm; F, K, M, N, O = 20 µm; G = 10 µm; H, J = 200 µm.

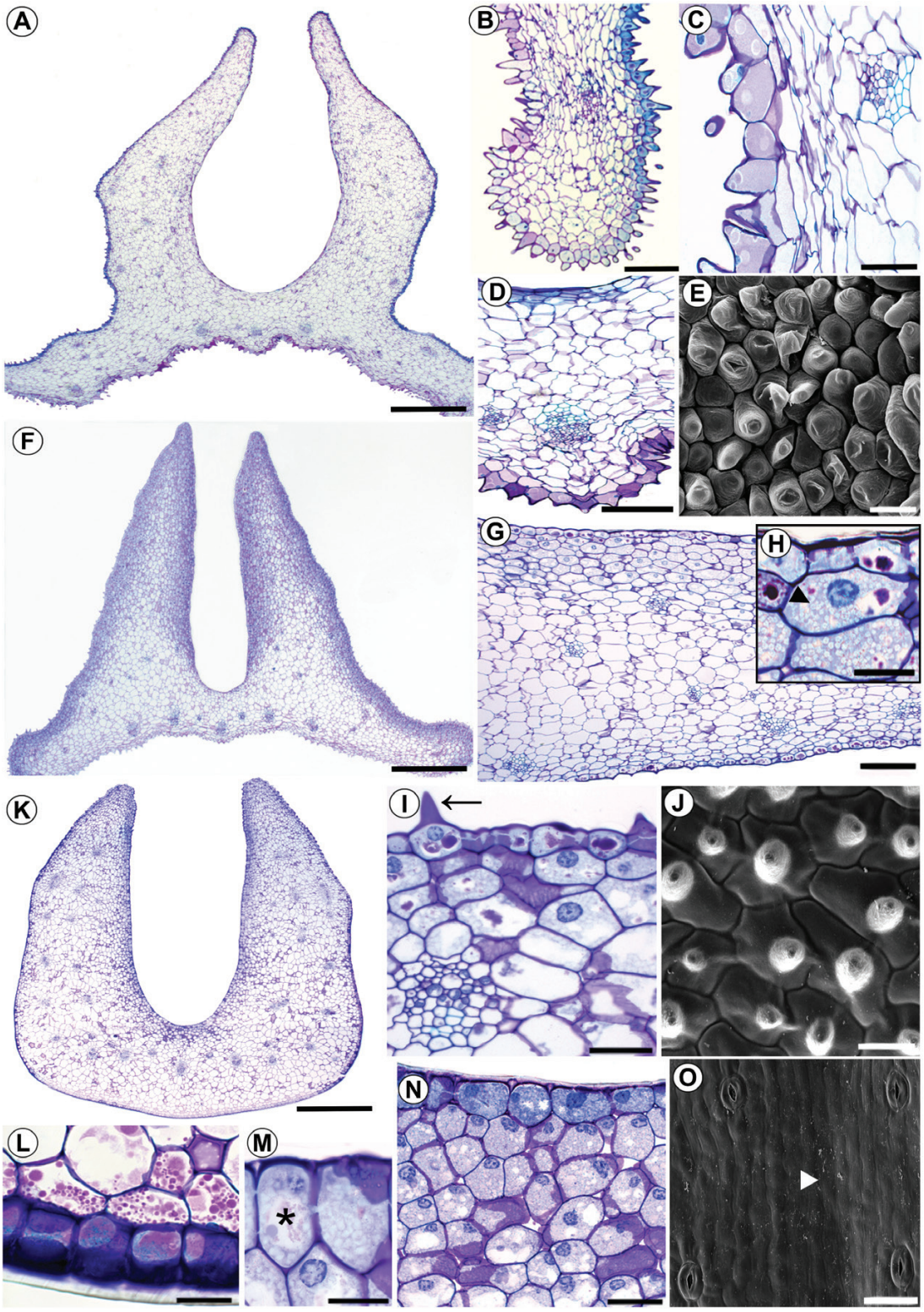

Figure 5. Osmophores and elaiophore in the labellum of *Gongora* species. Light microscopy unless otherwise stated. A–E, *G. jauariensis*. F–J, *G. pleiochroma*. K–O, *G. minax*. A, hypochile of *G. jauariensis* (cross-section). B, detail of horns. C, dorsal surface showing papillose cells of the epidermis. D, ventral surface without papillose cells and papillose dorsal surface. E, osmophore of labellum in *G. jauariensis* (SEM). F, hypochile of *G. pleiochroma* (cross-section). G, part of the

Cells of the secretory region of osmophores/elaiophores of *G. minax* have a voluminous nucleus (Fig. 8I), dense cytoplasm (Fig. 8I), developing vacuoles, vesicles, protoplasm with abundant amyloplasts and large intercellular spaces containing polysaccharides (Fig. 8I, 8K). Lipid drops occur both in the inner cytoplasm and near the periplasmic space (cytosol) (Fig. 8I–K). Mitochondria and numerous smooth and rough endoplasmic reticulum (Fig. 8J–K) are also observed. Branched plasmodesmata penetrate the walls between epidermal cells (Fig. 8I–J).

PHYTOCHEMISTRY

The components identified in the floral fragrance of *G. jauariensis* (Pa. 181), *G. pleiochroma* (Pa. 182) and *G. minax* (Pa. 175) with a percentage > 5% were as follows: Pa. 181 – (E) – β-farnesene and β-bisabolene, molecular mass (MM) = 208; Pa. 182 – eugenol and benzyl benzoate; and Pa. 175 – 1-hexadecanol acetate, 9,12-octadecadienoic acid (Z, Z), 1-octadecanol, docosane, behenic alcohol, 1-docosanol and tetracosane (Table 1).

DISCUSSION

Gongora pleiochroma, *G. jauariensis* and *G. minax* have similar anatomical features, especially the nectaries in the bracts, the digitiform trichomes along the epidermal surfaces of the bracts and sepals and the crystalliferous idioblasts (raphides) of calcium oxalate distributed in the mesophyll. The features of the osmophores in the labella and sepals are similar to those described for other species of Stanhopeinae (Vogel, 1990; Curry, 1991; Antón *et al.*, 2012; Casique *et al.*, 2018). After the scent was released and the nectar was exuded, euglossine bees and ants were present in these areas, and it was possible to identify these structures.

Osmophores or scent glands are important in maintaining plant-pollinator interactions, and in some plants they are the major producers and releasers of flower fragrance (Dudareva & Pichersky, 2006; Weimer *et al.*, 2009). Floral scent is the most important reward and the main attribute responsible for attracting male euglossine bees, which are major pollinators of Stanhopeinae (Gerlach, 2003; Antón *et al.*, 2012; Pansarin, Pansarin & Sazima, 2014; Adachi *et al.*, 2015). In some orchid species, these scents are volatilized mainly via diffusion through the cuticle (Stern, Curry & Pridgeon, 1987; Stpiczyńska, 2001); a similar process was observed in the three *Gongora* spp. analysed here.

Floral scents produced by osmophores are often comprised of isoprenoids, ketones, esters, terpenoid aldehydes, benzenoids and phenylpropanoids, which are derived from fatty acids, and several other nitrogen and sulphur compounds that often have low molecular weight, low polarity and low vapour pressure, which enables scent volatilization; in other words, they produce substances of all possible metabolic origins (Silva, 1990; Tölke *et al.*, 2019). In the Orchidaceae, the chemical composition of the floral scent in orchids pollinated by euglossine bees tends to be dominated by volatile monoterpenoids, sesquiterpenoids and aromatic compounds (Williams & Whitten, 1983). Terpenoids are comprised of isoprene units (Curry, 1987) and are primarily responsible for attracting male bees of the Euglossini.

Pollination behaviour and mechanisms carried out by these bees on the flowers of these *Gongora* spp. are similar to those previously described for the genus and for other species of Stanhopeinae (Dressler, 1968; Gerlach, 2011; Pansarin *et al.*, 2014; Adachi *et al.*, 2015; Casique *et al.*, 2018). Male euglossine bees scratch and collect this scent from osmophores, store it on specialized posterior tibias and possibly disperse and expose it to conspecific females (Eltz *et al.*, 1999; Zimmermann, Roubik & Eltz, 2006; Adachi *et al.*, 2015; Hetherington-Rauth & Ramírez, 2015; Nunes *et al.*, 2017).

Osmophores in the Orchidaceae are found almost exclusively on the labella (Vogel, 1990). The osmophores in *G. jauariensis*, *G. pleiochroma* and *G. minax* are found in the ventral and dorsal parts of the labellum (hypochile) and also on the sepals (adaxial surface). They are epidermal, with papillose cells in *G. jauariensis* and *G. pleiochroma* and non-papillose cells in *G. minax*. Osmophores can have other morphological features, e.g. they can be smooth or have multi- or unicellular trichomes. The secretory epidermal cells can have different shapes, with or

labellum showing the ventral and dorsal surfaces. H, detail of ventral surface, cells with numerous starch grains (arrow head). I, detail of dorsal surface with some papillose cells (arrows). J, osmophore of labellum in *G. pleiochroma* (SEM). K, hypochile of *G. minax* (cross-section). L, ventral surface (hypochile), with content visible in intercellular spaces. M, detail of epidermal cells in the ventral surface, evident lipid drops (*). N, dorsal surface (hypochile) and evident lipid drops in this area. O, ventral surface of labellum with osmophores/elaiophores in *G. minax*, sparse stomata (arrowhead), and epicuticular wax (arrowhead). Scale bars: A, K = 500 µm; B, H, L = 100 µm; C = 200 µm; D, F = 350 µm; E, I, J = 20 µm; G, M = 10 µm; N–O = 50 µm.

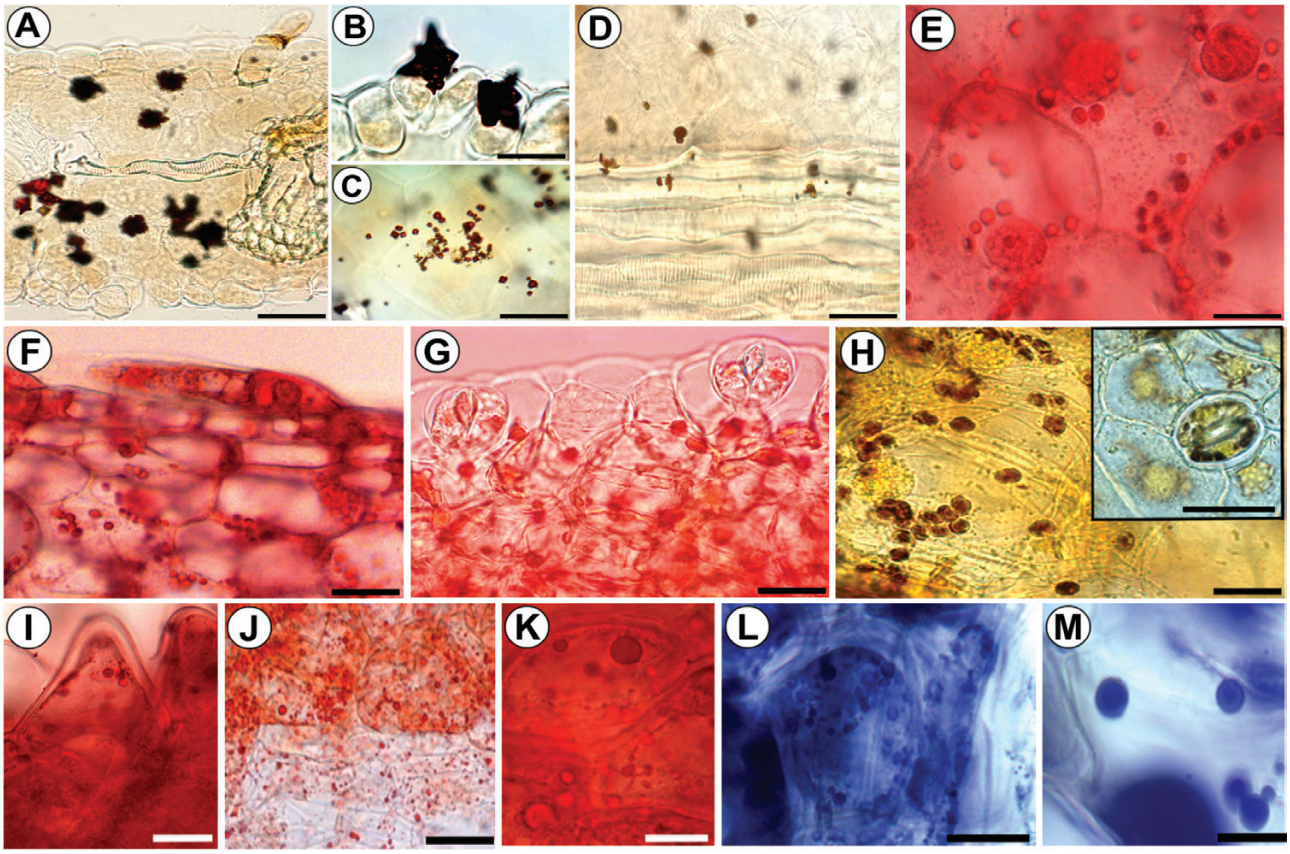

Figure 6. Histochemical analysis of *Gongora* species of the median regions (cross-section) of bracts (A–H) and sepals (I–M). A–D, Fehling reagent. A–B, mesophyll and stomata of *G. minax*. C–D, mesophyll of *G. jauariensis*. E–G, Ponceau xylidine. E–F, staining with xylidine revealed the presence of protein bodies in the mesophyll and trichome of *G. pleiochroma*. G, protein bodies in the stomata of *G. minax*. H, staining with Lugol reagent in the mesophyll and stomata of *G. jauariensis*. I–K, Sudan III. I, staining with Sudan III revealed the presence of lipid bodies in the sepals of *G. jauariensis*. J, mesophyll of *G. pleiochroma*. K, mesophyll of *G. minax*. L–M, staining with NADI reagent. L, mesophyll of *G. jauariensis*. M, mesophyll of *G. minax*. Scale bars: A = 50 μm; B–M = 10 μm.

without papillae (uni- or multicellular) or simply cubic (Vogel, 1990; Curry, 1991; Antón *et al.*, 2012; Casique *et al.*, 2018; Kettler *et al.*, 2019; Tölke *et al.*, 2019).

The features observed in the osmophores of sepals and labella of these *Gongora* spp. have similarities to previous descriptions of other taxa of Stanhopeinae, including *Gongora bufonia* Lindl., *S. grandiflora, Stanhopea oculata* Lindl., *Stanhopea wardii* Lodd. ex Lindl., *Sievekingia* Rchb.f. and *Cirrhaea* Lindl. (Stern *et al.*, 1987; Curry *et al.*, 1991; Davies & Turner, 2004; Ascensão *et al.*, 2005; Pansarin *et al.*, 2014; Adachi *et al.*, 2015). In other orchids, the osmophores may be located on the petal tips and ovary surface (Silveira, 2002; Kowalkowska, Kozieradzka-Kiszkurno & Turzyński, 2015).

Chemical analysis of the scent of these *Gongora* spp. revealed typical compounds of aromas usually found in other flowers of these genera, scents that are closely related to pollinator attraction (Hetherington-Rauth & Ramírez, 2015, 2016). Compounds such as eugenol, (E)-β-farnesene, β-bisabolene, docosane and tetracosane, all present in *G. pleiochroma*, *G. jauariensis* and *G. minax*, are similar to those in *Stanhopea* spp. (Gerlach, 2010; Casique *et al.*, 2018). With alcohol, tetradecyl and hexadecyl acetate, primary compounds common to the three species of *Gongora*, there are other substances that are often involved in attracting potential pollinator bees, including monoterpenes [α-pinene, β-pinene, sabinene, myrcene, limonene, eucalyptol (1,8-cineol) and ocimene] (Whitten & Williams, 1992).

Elaiophores are secretory structures that produce non-volatile oils that aid in the mutual relationship between oil-producing flowers and the bees that collect this oil, which are their potential pollinators (Vogel, 1974; Possobom & Machado, 2017). There are

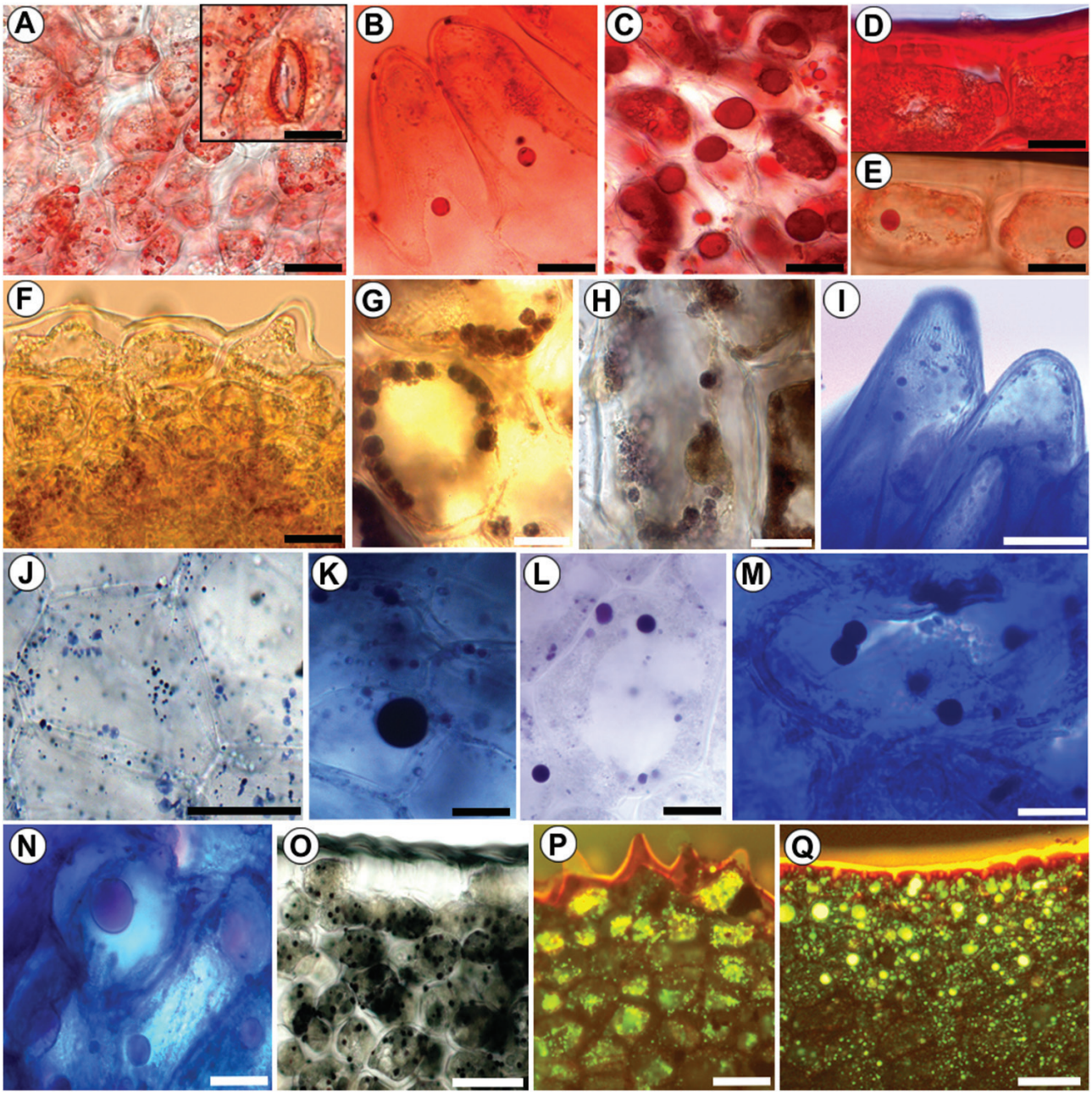

Figure 7. Labellum (hypochile) histochemical analysis of *Gongora* species. A, staining with Sudan III in the secretory parenchyma of *G. jauariensis*. B, papillose cells with Sudan III of *G. pleiochroma*. C–E, staining with Sudan III of *G. minax*. D–E, ventral surface and dorsal surface, respectively, of labellum of *G. minax* with Sudan III. F–G, starch grains (Lugol reagent) of *G. pleiochroma*. H, starch grains (Lugol reagent) of *G. minax*. I–J, essential oils (NADI reagent) *G. jauariensis* and *G. pleiochroma*, respectively. K, essential oils (NADI reagent) in *G. minax*. L, oil resin in *G. minax*. M, bodies of acid lipids (Nile blue sulphate) in *G. jauariensis*. N, bodies of neutral lipids (Nile blue sulphate) in *G. minax*. O, staining bodies with fatty acids (copper acetate/rubeanic acid) in the labellum of *G. minax*. P, labellum with neutral red in UV light of *G. jauariensis*. Q, labellum with neutral red in UV light of *G. minax*. Scale bars: A–N = 10 μm; O–Q = 20 μm.

two types of elaiophores (trichomatous and epidermal; Vogel, 1974). Trichomatous elaiophores are comprised of glandular trichomes or uni- or multicellular epidermal excrescences, where oil can be secreted and/or accumulated or can even be stored below the cuticle until it is removed by the anterior legs of bees.

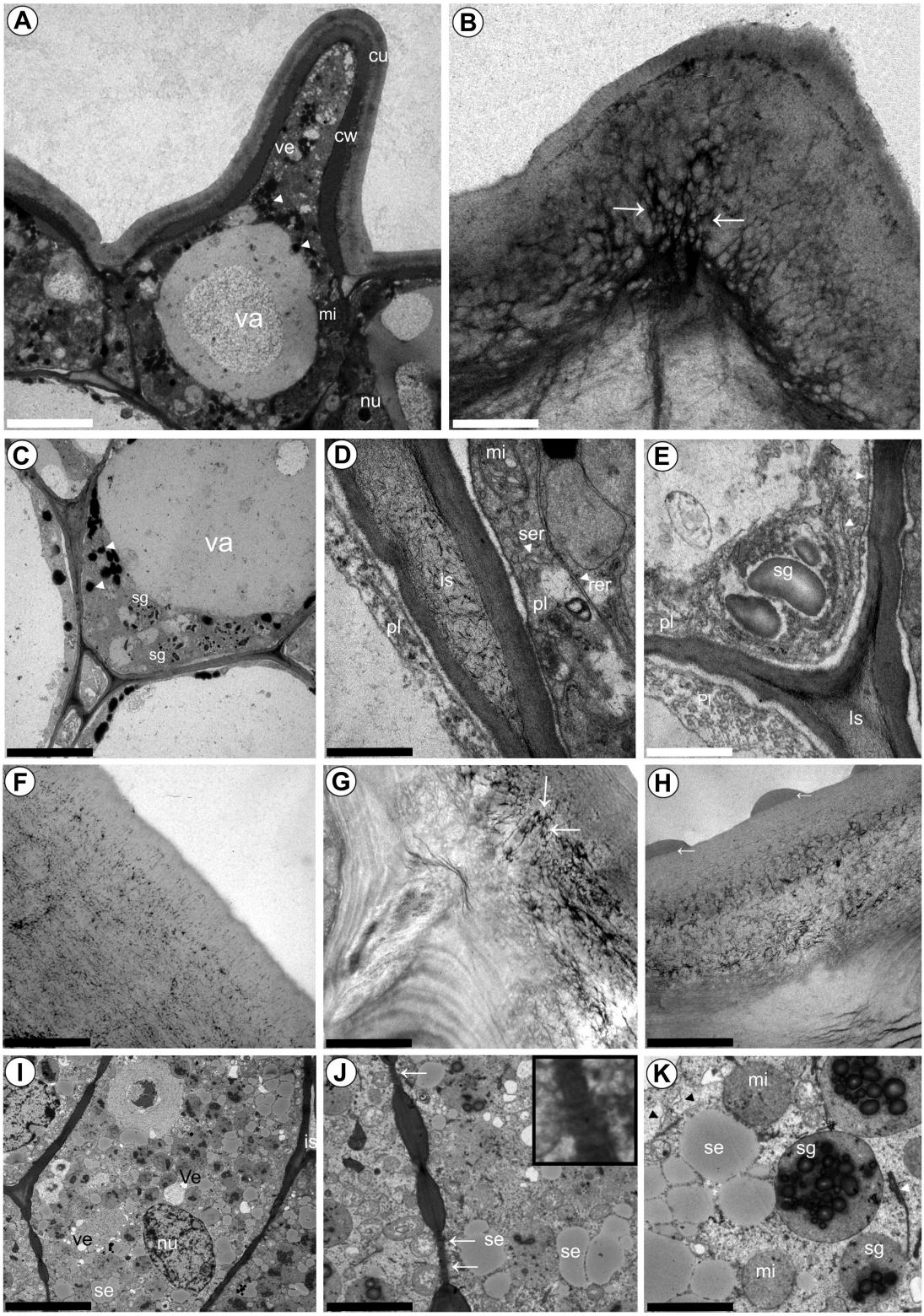

Figure 8. Analysis using transmission electron microscopy (TEM) of ventral and dorsal surfaces of labellum (hypochile) osmophores of the three *Gongora* species. A–E, *G. jauariensis* and *G. pleiochroma*. F–K, *G. minax*. A, secretory epidermal cell, papillose with thin periclinal wall on the dorsal surface of *G. jauariensis* with abundant cytoplasm, evident vacuole, numerous amyloplasts, lipid drops in vesicles (arrowhead), mitochondria and smooth (ser) and rough (rer) endoplasmic

Epidermal elaiophores are secretory epidermal cells covered by cuticle, under which the secretion can be stored (Vogel, 1974; Buchmann, 1987; Endress, 1994; Possobom & Machado, 2017; Tölke *et al.*, 2019). This second type is described here in the ventral area of the labella (hypochile) of *G. minax*, the same area where the osmophores are found.

We did not observe female bees in this study. Therefore, future investigations of ecological interactions with *G. minax* are required. These will enable us to clarify the importance of this oil for the bee and pollination, and thus confirm the role played by the elaiophore.

These structures were first described in the Malpighiaceae by Vogel (1969). In the Orchidaceae, elaiophores have been described in species of Oncidiinae (Whitten *et al.*, 2000), and *Zygostates* Lindl. and *Oncidium* Sw. (Vogel, 1974). Epidermal elaiophores can be found at the base of the labellum or above the callus and on lobes of the labellum in some Oncidiinae (Pacek & Stpiczyńska, 2007; Stpiczyńska, Davies & Gregg, 2007; Pacek *et al.*, 2012; Gomiz, Torretta & Aliscioni, 2013). They can be comprised of a cuboid cell layer (Singer & Cocucci, 1999; Pacek & Stpiczyńska, 2007; Pacek *et al.*, 2012; Davies, Stpiczyńska & Rawski, 2014) or palisade cells (Stpiczyńska & Davies, 2008; Gomiz *et al.*, 2013; Stpiczyńska *et al.*, 2013). The position and structure of the elaiophore and the degree of oil secretion vary according to the morphological group (Blanco *et al.*, 2013).

The elaiophores of *G. minax* contained mainly fatty acids and/or glyceride derivatives such as 1-hexadecanol, acetate, behenic alcohol and 1-docosanol, which are commonly reported in phytochemical studies of elaiophores (Vogel, 1974; Buchmann, 1987; Cocucci, 1991; Reis *et al.*, 2000; Reis *et al.*, 2007; Vogel, 2009). Other, minor constituents reported include aldehydes, amino acids, carbohydrates, carotenoids, hydrocarbons, isoprenoid compounds, ketones, phenolic compounds, saponins and terpenes (Vogel, 1974; Simpson & Neff, 1981; Buchmann, 1987; Reis *et al.*, 2000; Reis *et al.*, 2006). Elaiophores produce not only fatty acids but also acid mucilage, which with the oil makes the secretion more fluid and facilitates collection by bees (Pansarin *et al.*, 2009). The presence of nectar, lipids and sugar traces in some floral oils (Vogel, 1990; Davies *et al.*, 2003) and the presence of terpenoids in nectar (Davies, Stpiczyńska & Gregg, 2005) of some species may indicate that the elaiophores are derived from nectaries (Stpiczyńska *et al.*, 2007).

The first ultrastructural analyses of osmophores with a granulocrine secretion in the Orchidaceae were performed with *Restrepia* Kunth and *Scaphosepalum* Pfitzer (Pridgeon & Stern, 1983, 1985). Among species of Stanhopeinae, the analysis was initially performed with *S. oculata*, *S. wardii* and *S. graveolens* Lindl.; the major organelles observed were mitochondria, amyloplasts, elaioplasts and smooth and rough endoplasmic reticulum (Stern *et al.*, 1987; Antón *et al.*, 2012). *Gongora bufonia*, however, showed certain particularities, such as branched plasmodesmata, a reticulated cuticle and the apparent absence of rough endoplasmic reticulum (Adachi *et al.*, 2015). In other species, microchannels occur, having been described in *Bulbophyllum wendlandianum* (Kraenzl.) Dammer and *Bulbophyllum weberi* Ames (Kowalkowska *et al.*, 2015; Kowalkowska, Turzyński & Kozieradzka-Kiszkurno, 2017). In *G. jauariensis*, *G. pleiochroma* and *G. minax*, the structures are similar to those found in *Stanhopea* and *G. bufonia*. These cellular components, smooth and rough endoplasmic reticulum, mitochondria and plastids are closely involved in fragrance synthesis, which is produced and exuded by floral osmophores, and are commonly reported in osmophores of orchids and other plants (Stern *et al.*, 1987; Curry *et al.*, 1991; Stpiczyńska, 1993; Effemert *et al.*, 2006; Kowalkowska *et al.*, 2015; Stpiczyńska *et al.*, 2018; Paiva *et al.*, 2019; Tölke *et al.*, 2019).

The surface of the labellum (hypochile) of *G. minax* is covered with grains of epicuticular wax, as in *G. bufonia*, which, according to Adachi *et al.* (2015), may aid in pollination by causing the pollinator to slip and fall when positioning on and grasping the labellum; this would make it fall onto the column, thus removing the pollinarium. The flower morphology provides this pollination mechanism characteristic of the *Gongora* subgenera *Gongora* and *Portentosa* (Gerlach, 2009).

The starch grains in the osmophore cells of these species are a common feature of odoriferous glands (Stern *et al.*, 1987; Curry *et al.*, 1991; Pansarin *et al.*, 2009), since

reticula. B, cuticle of *G. pleiochroma* presenting a well-developed net of microchannels (arrows). C, In *G. pleiochroma*, amyloplasts containing visible starch grains, well-developed vacuoles, and lipid drops near of starch grains (arrowhead). D, In *G. jauariensis*, smooth and rough endoplasmic reticula, mitochondria and large intercellular spaces (Is). E, In *G. jauariensis*, detail of amyloplast containing starch grains and smooth endoplasmic reticulum (arrowhead). F, ventral surface of labellum with thick cuticle. G, outer periclinal wall polylamellate with microchannels (arrows). H, deposit of epicuticular wax (arrows) on the ventral surface. I, secretory cells of epidermis on the ventral surface. J, branched plasmodesmata (arrows) going through intercellular walls and detail. K, abundant lipid drops, amyloplasts containing starch grains, mitochondria, and smooth (black head arrow) and rough (white head arrow) endoplasmic reticula. Scale bars: A = 10 µm; B, G, H, K = 2 µm; C, J = 5 µm; D, F = 0.5 µm; E = 1 µm; I = 20 µm. For key, see Fig. 1.

Table 1. Analysis of the floral fragrance of *Gongora* species. *G. jauariensis* (Pa - 181), *G. pleiochroma* (Pa - 182) and *G. minax* (Pa - 175) (%)

RI	Constituents	Characterization	Pa-175	Pa-181	Pa-182
2086	[2-(2-Hydroxyphenyl)cyclopropyl](phenyl)methanone	Acetone	-	-	1.73
2170	Octadeca-(3Z,13Z)-dien-1-yl acetate	Acetone	-	0.46	-
1596	2,2,4-Trimethyl-1,3-pentanediol diisobutyrate	Alcohol	-	0.36	0.39
1634	α-Acorenol	Alcohol	-	0.33	-
62.499	1-Tricosanol	Alcohol	1.19	-	-
811	Hexanal	Aldehyde	-	0.27	3.60
1045	Phenylacetaldehyde	Aldehyde	-	0.96	1.49
1106	n-Nonanal	Aldehyde	-	1.97	2.09
1161	1,3,5,7-Cyclooctatetraene-1-carboxaldehyde	Aldehyde	-	0.16	-
1208	n-Decanal	Aldehyde	-	0.14	-
1273	(E)-Cinnamaldehyde	Aldehyde	-	-	0.44
820	Butyl-Acetate	Carboxylic Acid	-	0.77	-
1409	Methyl-Eugenol	Carboxylic Acid	-	1.83	-
1774	**Benzyl benzoate**	**Carboxylic Acid**	**-**	-	**60.63**
34.904	Dodecyl acetate	Carboxylic Acid	0.46	-	-
1877	Phthalic acid, isobutyl propyl ester	Ester	-	0.13	-
1968	Hexadecanoic acid	Fatty acid	-	0.62	-
2000	Ethyl hexadecanoate	Fatty acid	-	0.09	-
44.627	n-Hexadecanoic acid	Fatty acid	3.63	-	-
49.403	9-Octadecenoic acid (Z)-	Fatty acid	3.09	-	-
49.969	**9,12-Octadecadienoic acid (Z,Z)-**	**Fatty acid**	**7.09**	-	-
42.018	n-Hexadecanol	Fatty Alcohols	0.97	-	-
54.055	1-Octadecanol	Fatty Alcohols	5.19	-	-
59.496	**1-Docosanol**	**Fatty Alcohols**	**20.46**	-	-
64.961	1-Tetracosanol	Fatty Alcohols	1.32	-	-
46.178	**1-Hexadecanol, acetate**	**Fatty Esters**	**14.74**	-	-
52.234	Octadecyl acetate	Fatty Esters	1.03	-	-
1389	(E)-β-Damascenone	Hydrocarbon	-	0.06	-
1420	cis-α-Bergamotene	Hydrocarbon	-	0.42	-
1440	*trans*-α-Bergamotene	Hydrocarbon	-	0.86	-
39.581	1-Octadecene	Hydrocarbon	3.16	-	-
54.843	**Docosane**	**Hydrocarbon**	**5.98**	-	-
60.185	**Tetracosane**	**Hydrocarbon**	**12.04**	-	-
62.770	Pentacosane	Hydrocarbon	1.86	-	-
65.305	Hexacosane	Hydrocarbon	1.25	-	-
2305	Tricosane	Hydrocarbon	-	1.12	0.26
2405	Tetracosane	Hydrocarbon	-	0.34	-
1187	Naphthalene	Hydrocarbon	-	0.92	-
1292	Safrole	Hydrocarbon	-	0.11	2.27
1362	**Eugenol**	**Monoterpene**	**-**	0.29	**18.45**
7.432	Cineole<dehydro-1,8->	Monoterpene	0.22	-	-
8.293	α-Terpinene	Monoterpene	1.32	-	-
9.770	γ-Terpinene	Monoterpene	1.32	-	-
10.779	Terpinolene	Monoterpene	0.54	-	-
8.712	Sylvestrene	Monoterpene	0.56	-	-
11.346	Linalool	Monoterpene	0.49	-	-
13.389	Limonene oxide<cis->	Monoterpene	0.31	-	-
14.817	Thujone<trans->	Monoterpene	0.7	-	-
15.309	α-Terpineol	Monoterpene	0.94	-	-
16.490	Verbenyl acetate<trans->	Monoterpene	0.58	-	-
19.321	Cymen-8-ol <para->	Monoterpene	0.21	-	-

Table 1. Continued

RI	Constituents	Characterization	Pa-175	Pa-181	Pa-182
1380	α-Copaene	Sesquiterpene	-	-	0.31
1425	(E)-Caryophyllene	Sesquiterpene	-	-	0.37
1440	(Z)-β-Farnesene	Sesquiterpene	-	-	0.07
1461	**(E)-β-Farnesene**	**Sesquiterpene**	-	**5.15**	0.31
1444	β-Dihydroionone	Sesquiterpene	-	0.08	-
1448	Sesquisabinene	Sesquiterpene	-	0.2	-
1484	γ-Curcumene	Sesquiterpene	-	0.49	-
1487	α-Curcumene	Sesquiterpene	-	0.24	-
1517	β-Curcumene	Sesquiterpene	-	0.61	-
1528	β-Sesquiphellandrene	Sesquiterpene	-	4.72	-
1565	(E)-Nerolidol	Sesquiterpene	-	0.89	-
1630	Hinesol	Sesquiterpene	-	0.15	-
1515	**β-Bisabolene**	**Sesquiterpene**	-	**39.0**	0.5
1615	α-Bisabolol	Sesquiterpene	-	0.4	-
1676	epi-β-Bisabolol	Sesquiterpene	-	0.22	-
1693	epi-α-Bisabolol	Sesquiterpene	-	0.16	-
8.564	Cymene<ortho->	Terpene	0.27	-	-
14.669	Terpinen-4-ol	Terpene	0.92	-	-
1457	Geranylacetone	Terpene	-	0.16	-
1492	(E)-β-Ionone	Terpene	-	0.89	0.33
1500	α-Zingiberene	Terpene	-	0.61	-
1319	N.I.		-	3.84	4.81
1588	***MM=208**		**-**	**24.76**	**-**
31.457	RT:31.457		0.13	-	-
39.876	RT:39.876		0.19	-	-
41.181	RT:41.181		0.15	-	-
41.304	RT:41.304		0.25	-	-
44.529	RT:44.529		0.41	-	-
48.861	RT:48.861		0.20	-	-
49.034	RT:49.034		0.25	-	-
50.732	RT:50.732		0.93	-	-
50.905	RT:50.905		0.54	-	-
51.618	RT:51.618		0.23	-	-
54.252	RT:54.252		0.24	-	-
56.837	RT:56.837		0.42	-	-
57.576	RT:57.576		0.32	-	-
59.348	RT:59.348		0.06	-	-
59.693	RT:59.693		0.61	-	-
60.628	RT:60.628		0.13	-	-
61.490	RT:61.490		0.35	-	-
61.711	RT:61.711		0.72	-	-
63.951	RT:63.951		0.14	**-**	**-**
64.591	RT:64.591		0.30	-	-
64.690	RT:64.690		0.08	-	-
65.084	RT:65.084		0.18	-	-

Bold indicates emphasis on the class of chemical compounds analysed.

*RI = retention index; N.I = not identified in the literature; MM = molecular mass; RT = retention time.

starch is used as an energy source for the production of nectar or scent (Vogel, 1990; Effemert *et al.*, 2006). These starch agglomerations decrease as volatile evaporation occurs, along with increased vacuole volume and reduced cytoplasm; however, a thin peripheral cytoplasm layer remains, as do some large lipid drops, a few amyloplasts, mitochondria and smooth and rough endoplasmic reticulum (Pridgeon & Stern, 1983; Effemert *et al.*, 2006).

As seen by *in situ* histochemical analysis, the main classes of metabolites are the terpenoids in the three *Gongora* spp. and free fatty acids, especially in *G. minax*, as confirmed by the list of compounds obtained from phytochemical analysis of the labella (Table 1). The labellar secretion of *G. minax* is a heterogeneous mixture, containing mainly lipophilic substances, including a high content of free fatty acids and terpenoids. Free fatty acids are the most common components found in floral oils of the elaiophores (Vogel, 1974; Reis *et al.*, 2006; Possobom & Machado, 2017). The intense staining of the floral tissue with reagents such as neutral red help in osmophore identification (Vogel, 1990; Pansarin & Pansarin, 2011; Francisco & Ascensão, 2013). The stains Sudan black, Sudan III and Sudan IV are useful for the detection of triacylglycerides and total lipids bound to proteins (Effemert *et al.*, 2006). Nile blue sulphate indicates the presence of different lipids such as acid and neutral lipids, and NADI aids in terpenoid identification (Effemert *et al.*, 2006; Demarco, 2017). All these tests reacted positively, indicating that this secretion is compatible with that secreted by osmophores. Aside from staining, identifying volatile compounds by means of a gas chromatography mass spectrometer (GC-MS) is essential for osmophore identification (Effemert *et al.*, 2006).

Nectaries were also observed at the base of the bract in the preanthetic and anthetic stages in *Gongora*, as in *S. grandiflora* (Casique *et al.*, 2018). Ants were observed on the bract, even with anthetic flowers and with bees present. This ant foraging is similar to that reported for *Epidendrum denticulatum* Barb.Rodr.; the ants do not interfere with pollinator behaviour (Almeida & Figueiredo, 2003; Gerlach, 2011; Leitão *et al.*, 2014). This association with ants also has been reported in *Coryanthes* Hook. and, recently, in *S. grandiflora*, where ants feed on nectar from extrafloral nectaries and can use the plant to build their nests while defending the plants from herbivores and fertilizing them with vertebrate faeces (Gerlach, 2011; Casique *et al.*, 2018). This nutrient substance offered by ants allows the plants to grow more rapidly (Gerlach, 2011; Gegenbauer *et al.*, 2012).

In conclusion, by means of anatomical, histochemical and phytochemical analyses, we observed the osmophores commonly described for Stanhopeinae. These structures are involved in the attraction and reward of pollinators, i.e. male euglossine bees. In *G. minax*, the labellum (hypochile) showed chemical and structural characteristics of the elaiophore and osmophore. It can thus be assumed that the same structure may function as both an osmophore and elaiophore. The elaiophore described here was characterized mainly through chemical and TEM analyses. Elaiophores are commonly described in the Malpighiaceae, Iridaceae and other Orchidaceae; the main ecological function of the secreted oils is their use by female euglossine bees to coat the wall of their nest. Further studies on the floral biology of this species will be needed to identify the female bee or the true function of this exuded oil for the pollination process. Interactions between foraging ants and nectaries of bracts are reported for the first time in *Gongora*. However, we emphasize the need for further studies of these nectaries, using TEM to elucidate the secretion processes.

ACKNOWLEDGEMENTS

The authors are grateful to the Biodiversity Authorization and Information System (Sisbio) for providing the sampling permit; we thank Luiz Otávio Adão and João Batista for their collaboration in the fieldwork. J.V.C.T. thanks the Coordenação de Aperfeiçoamento de Pessoal de Nível Superior (CAPES) for granting a scholarship and supporting our research and the Museu Paraense Emílio Goeldi and Universidade Federal do Rio Grande do Sul, especially the Laboratory of Plant Anatomy (LAVeg) and Center of Microscopy and Microanalysis (Centro de Microscopia e Microanálise – CME), for the support provided to carry out this study.

REFERENCES

Adachi S, **Machado S**, **Guimarães E. 2015.** Structural and ultrastructural characterization of the floral lip in *Gongora bufonia* Lindl. (Orchidaceae): understanding the slip-and-fall pollination mechanism. *Botany* **93:** 759–768.

Adams P. 2007. *Identification of essential oil components by gas chromatography / mass spectrometry*, *4th edn*. Carol Stream: Allured Publishing.

Aguiar JMRBV, **Pasarin LM**, **Ackerman JD**, **Pasarin ER. 2012.** Biotic vs. abiotic pollination in *Oeceoclades maculata* (Lindl.) Lindl. (Orchidaceae: Epidendroideae). *Plant Species Biology* **27:** 86–95.

Almeida AM, **Figueiredo RA. 2003.** Ants visit nectaries of *Epidendrum denticulatum* (Orchidaceae) in a Brazilian rainforest: effects on herbivory and pollination. *Brazilian Journal of Biology* **63:** 551–558.

Antoń S, **Kamińska M**, **Stpiczyńska M. 2012.** Comparative structure of the osmophores in the flower of *Stanhopea graveolens* Lindley and *Cycnoches chlorochilon* Klotzsch (Orchidaceae). *Acta Agrobotanica* **65:** 11–22.

Ascensão L, **Francisco A**, **Cotrim H**, **Pais MS. 2005.** Comparative structure of the lip in *Ophrys fusca* and *O. lutea* (Orchidaceae). *American Journal of Botany* **92:** 1059–1067.

Bembé B. 2004. Functional morphology in male euglossine bees and their ability to spray fragrances (Hymenoptera, Apidae, Euglossini). *Apidologie* **35:** 283–291.

Blanco MA, **Davies KL**, **Stpiczyńska M**, **Carlsward BS**, **Ionta GM**, **Gerlach G. 2013.** Floral elaiophores in *Lockhartia* hook. (Orchidaceae: Oncidiinae): their distribution, diversity and anatomy. *Annals of Botany* **112:** 1775–1791.

Buchmann SL. 1987. The ecology of oil flowers and their bees. *Annual Review of Ecology, Evolution, and Systematics* **18:** 343–369.

Cain AJ. 1947. The use of Nile blue in the examination of lipids. *Quarterly Journal of Microscopical Science* **88:** 383–392.

Cardoso-Gustavson P, **Campbell LM**, **Mazzoni-Viveiros SC**, **DE Barros F. 2014.** Floral colleters in Pleurothallidinae (Epidendroideae: Orchidaceae). *American Journal of Botany* **101:** 587–597.

Casique JV, **Silva EF**, **Andrade EHA**, **Mastroberti AA**, **Aguiar-Dias ACA. 2018.** Anatomical analyses of floral and extrafloral secreting structures indicate the presence of nectaries and colleters in *Stanhopea grandiflora* Lindl. *Brazilian Journal of Botany* **41:** 725–738.

Chase MW, **Cameron KM**, **Barrett RL**, **Freudenstein JV. 2003.** DNA data and Orchidaceae systematics: a new phylogenetic classification. In: Dixon KW, Kell SP, Barrett RL, Cribb PJ, eds. *Orchid conservation*. Kota Kinabalu: Natural History Publications, 69–89.

Chase MW, **Cameron KM**, **Freudenstein JV**, **Pridgeon AM**, **Salazar G**, **van den Berg C**, **Schuiteman A. 2015.** An updated classification of Orchidaceae. *Botanical Journal of the Linnean Society* **177:** 151–174.

Cocucci AA. 1991. Pollinaton biology of *Nierembergia* (Solanaceae). *Plant Systematics and Evolution* **174:** 17–35.

Curry KJ. 1987. Initiation of terpenoid synthesis in osmophores of *Stanhopea anfracta* (Orchidaceae): a cytochemical study. *American Journal of Botany* **74:** 1332–1338.

Curry KJ, **McDowell LM**, **Judd WS**, **Stern WL. 1991.** Osmophores, floral features, and systematics of *Stanhopea* (Orchidaceae). *American Journal of Botany* **78:** 610–623.

David R, **Carde JP. 1964.** Coloration différentielle dês inclusions lipidique et terpeniques dês pseudophylles du pin maritime au moyen du reactif Nadi. *Comptes Rendus Hebdo Séances de l'Académie dês Sciences Paris* **258:** 1338–1340.

Davies KL, **Stpiczyńska M. 2012.** Comparative labellar anatomy of resin-secreting and putative resin-mimic species of *Maxillaria s.l.* (Orchidaceae: Maxillariinae). *Botanical Journal of the Linnean Society* **170:** 405–435.

Davies KL, **Stpiczyńska M. 2017.** Comparative floral micromorphology and the ultrastructural basis of fragrance production in pseudocopulatory *Mormolyca s.s.* and non-pseudocopulatory *Maxillaria* section *Rufescens s.s.* (Orchidaceae). *Botanical Journal of the Linnean Society* **185:** 81–112.

Davies KL, **Stpiczyńska M**, **Gregg A. 2005.** Nectar-secreting floral stomata in *Maxillaria anceps* Ames & C.Schweinf. (Orchidaceae). *Annals of Botany* **96:** 217–227.

Davies KL, **Stpiczyńska M**, **Rawski M. 2014.** Comparative anatomy of floral elaiophores in *Vitekorchis* Romowicz & Szlach., *Cyrtochilum* Kunth and a florally dimorphic species of *Oncidium* Sw. (Orchidaceae: Oncidiinae). *Annals of Botany* **113:** 1155–1173.

Davies KL, **Turner MP. 2004.** Morphology of floral papillae in *Maxillaria* Ruiz & Pav. (Orchidaceae). *Annals of Botany* **93:** 75–86.

Davies KL, **Turner MP**, **Gregg A. 2003.** Lipoidal labellar secretions in *Maxillaria* Ruiz & Pav. (Orchidaceae). *Annals of Botany* **91:** 439–446.

Demarco D. 2017. Histochemical analysis of plant secretory structures. In: Pellicciari C, Biggiogera M, eds. *Histochemistry of single molecules – methods and protocols*. Pavia: Human Press, 313–330.

Dressler RL. 1968. Pollination by Euglossini bees. *Evolution* **22:** 202–210.

Dressler RL. 1982. Biology of the orchid bees (Euglossini). *Annual Review of Ecology and Systematics* **13:** 373–394.

Dressler RL. 1993. *Phylogeny and classification of the orchid family*. Portland: Dioscorides Press.

Dudareva N, **Pichersky E. 2006.** *Biology of floral scent*. Boca Raton: Taylor and Francis.

Effemert U, **Buss D**, **Rohrbeck D**, **Piechulla B. 2006.** Localization of the synthesis and emission of scent compounds within the flower. In: Dudareva N, Pichersky E, eds. *Biology of floral scent*. London: CRC Press, 105–124.

Eltz T, **Whitten WM**, **Roubik DW**, **Linsenmair KE. 1999.** Fragrance collection, storage, and accumulation by individual male orchid bees. *Journal of Chemical Ecology* **25:** 157–176.

Endress PK. 1994. *Diversity and evolutionary biology of tropical flowers*. Cambridge: Cambridge University Press.

Fahn A. 1979. Ultrastructure of nectaries in relation to nectar secretion. *American Journal of Botany* **57:** 977–985.

Flora do Brasil. **2020 (in construction).** Flora do Brasil. Jardim Botânico do Rio de Janeiro. Available at: http://floradobrasil.jbrj.gov.br/. Accessed 12 August 2019.

Francisco A, **Ascensão L. 2013.** Structure of the osmophore and lip micromorphology in the sexually deceptive orchids *Ophrys bombyliflora* and *Ophrys tenthredinifera* (Orchidaceae). *International Journal of Plant Science* **174:** 619–636.

Franken EP, **Pansarin LM**, **Pansarin ER. 2016.** Osmophore diversity in the *Catasetum cristatum* alliance (Orchidaceae: Catasetinae). *Lankesteriana* **16:** 317–327.

Ganter P, **Jollès G. 1969.** *Histologie normale et pathologique*, **Vol. 1**. Paris: Gauthier-Villars.

Ganter P, **Jollès G. 1970.** *Histologie normale et pathologique*, **Vol. 2**. Paris: Gauthier-Villars.

Gegenbauer C, **Mayer VE**, **Zotz G**, **Richter A. 2012.** Uptake of ant-derived nitrogen in the myrmecophytic orchid *Caularthron bilamellatum*. *Annals of Botany* **110:** 757–765.

Gerlach G. 2003. La subtribu Stanhopeinae: sus notables mecanismos de polinización, la química de sus aromas florales e implicaciones en sistemática y taxonomía. *Lankesteriana* **7:** 104–106.

Gerlach G. 2010. Stanhopeinae Mesoamericanae, V. El aroma floral de las stanhopeas de Mexico. *Lankesteriana* **9:** 431–442.

Gerlach G. 2011. The genus *Coryanthes*: a paradigm in ecology. *Lankesteriana* **11:** 253–264.

Gerlach G, **Dressler RL. 2003.** Stanhopeinae Mesoamericanae. *Lankesteriana* **8:** 23–30.

Gerlach G, **Whitten WM. 2009.** Stanhopeinae. In: Pridgeon, AM, Cribb PJ, Chase MW, Rasmussen FN. *Genera orchidacearum*, **Vol. 5**. Oxford, New York: Oxford University Press, 394–399.

Gerrits PO, **Smid L. 1983.** A new less toxic polymerization system for the embedding of soft tissues in glycol methacrylate and subsequent preparing of serial sections. *Journal of Microscopy* **132:** 81–85.

GersterbergerP, **LeinsP. 1978.** Rasterelektronmikroskopische Untersuchungen an Blütenknospen von *Physalis philadelphica* (Solanaceae). Anwendung einer neuen Präparationsmethode. *Berichte der Deutschen Botanischen Gesellschaft* **91:** 381–387.

Gomiz NE, **Torretta JP**, **Aliscioni SS. 2013.** Comparative anatomy of elaiophores and oil secretion in the genus *Gomesa* (Orchidaceae). *Turkish Journal of Botany* **37:** 859–871.

Hanaichi T, **Sato T**, **Iwamoto T**, **Malavasi-Yamashiro J**, **Hoshino M**, **Mizuno N. 1986.** A stable lead by modification of Sato's method. *Journal of Electron Microscopy* **35:** 304–306.

Hetherington-Rauth MC, **Ramírez SR. 2015.** Evolutionary trends and specialization in the euglossine bee-pollinated orchid genus *Gongora*. *Annals of the Missouri Botanical Garden* **100:** 271–299.

Hetherington-Rauth MC, **Ramírez SR. 2016.** Evolution and diversity of floral scent chemistry in the euglossine bee-pollinated orchid genus *Gongora*. *Annals of Botany* **118:** 135–148.

Jennings W, **Shibamoto T. 1980.** *Qualitative analysis of flavor and fragrance volatiles by glass capillary gas chromatography*. London: Academic Press.

Johansen DA. 1940. *Plant microtechnique*. New York: McGraw-Hill.

Kettler BA, **Solís SM**, **Ferrucci MS. 2019.** Comparative survey of secretory structures and floral anatomy of *Cohniella cepula* and *Cohniella jonesiana* (Orchidaceae: Oncidiinae). New evidences of nectaries and osmophores in the genus. *Protoplasma* **256:** 703–720.

Kirk-Junior PW. 1970. Neutral red as a lipid fluorochrome. *Stain Technology* **45:** 1–4.

Kowalkowska AK, Kozieradzka-Kiszkurno M, Turzyński S. 2015. Morphological, histological and ultrastructural features of osmophores and nectary of *Bulbophyllum wendlandianum* (Kraenzl.) Dammer (*B.* section *Cirrhopetalum* Lindl., Bulbophyllinae Schltr., Orchidaceae). *Plant Systematics and Evolution* **301:** 609–622.

Kowalkowska AK, **Turzyński S**, **Kozieradzka-Kiszkurno M. 2017.** Floral structure of two species of *Bulbophyllum* section *Cirrhopetalum* Lindl.: *B. weberi* Ames and *B. cumingii* (Lindl.) Rchb.f. (Bulbophyllinae Schltr., Orchidaceae). *Protoplasma* **254:** 1431–1449.

Leitão CAE, **Dolder MAH**, **Cortelazzo AL. 2014.** Anatomy and histochemistry of the nectaries of *Rodriguezia venusta* (Lindl.) Rchb.f. (Orchidaceae). *Flora* **209:** 233–243.

Likens ST, **Nickerson GB. 1964.** Detection of certain hop oil constituents in brewing products. *Journal of the American Society of Brewing Chemists* **22:** 5–13.

McDowell EM, **Trump B. 1976.** Histological fixatives for diagnostic light and electron microscopy. *Archives of Pathology & Laboratory Medicine* **100:** 405–414.

Melo MC, **Borba EL**, **Paiva EAS. 2010.** Morphological and histological characterization of the osmophores and nectaries of four species of *Acianthera* (Orchidaceae: Pleurothallidinae). *Plant Systematics and Evolution* **286:** 141–151.

Metcalfe C, **Chalk L. 1950.** *Anatomy of the dicotyledons*. Oxford: Clarendon Press.

Mondello L. 2011. *Flavors and fragrances of natural and synthetic compounds*, *2nd edn*. New Jersey: Wiley.

Neubig KM, **Carlsward BS**, **Whitten WM**, **Williams NH. 2015.** Nectary structure and nectar in *Sobralia* and *Elleanthus* (Sobralieae: Orchidaceae). *Lankesteriana* **15:** 113–127.

Nunes CEP, **Castro MD**, **Galetto L**, **Sazima M. 2013.** Anatomy of the floral nectary of ornithophilous *Elleanthus brasiliensis* (Orchidaceae: Sobralieae). *Botanical Journal of the Linnean Society* **171:** 764–772.

Nunes CEP, **Gerlach G**, **Bandeira KDO**, **Gobbo-Neto L**, **Pansarin ER**, **Sazima M. 2017.** Intriguing chemical similarity: floral scents of *Catasetum cernuum* and *Gongora bufonia* suggest convergent evolution to a unique pollination niche. *Flora* **232:** 207–216.

O'Brien TP, **Feder N**, **McCully ME. 1964.** Polychromatic staining of plant cell walls by toluidine blue. *Protoplasma* **59:** 368–373.

Pacek A, **Stpiczyńska M. 2007.** The structure of elaiophores in *Oncidium cheirophorum* Rchb.f. and *Ornithocephalus kruegeri* Rchb.f. (Orchidaceae). *Acta Agrobotanica* **60:** 9–14.

Pacek A, **Stpiczyńska M**, **Davies KL**, **Szymczak G. 2012.** Floral elaiophore structure in four representatives of the *Ornithocephalus* clade (Orchidaceae: Oncidiinae). *Annals of Botany* **110:** 809–820.

Paiva EAS, **Dötterl S**, **De-Paula OC**, **Schlindwein C**, **Souto LS**, **Vitarelli NC**, **Silva CI**, **Mateus S**, **Alves-dos-Santos I**, **Oliveira DMT. 2019.** Osmophores of *Caryocar brasiliense* (Caryocaraceae): a particular structure of the androecium that releases an unusual scent. *Protoplasma* **256:** 971–981.

Pansarin ER, **Pansarin LM. 2011.** Reproductive biology of *Trichocentrum pumilum*: an orchid pollinated by oil-collecting bees. *Plant Biology* **13:** 576–581.

Pansarin LM, **Castro M**, **Sazima M. 2009.** Osmophore and elaiophores of *Grobya amherstiae* (Catasetinae, Orchidaceae) and their relation to pollination. *Botanical Journal of the Linnean Society* **159:** 408–415.

Pansarin ER, **Salatino A**, **Pansarim LM**, **Sazima M. 2012.** Pollination systems in Pogonieae (Orchidaceae: Vanilloideae): a hypothesis of evolution among reward and rewardless flowers. *Flora* **207:** 849–861.

Pansarin LM, **Pansarin ER**, **Sazima M. 2014.** Osmophore structure and phylogeny of *Cirrhaea* (Orchidaceae, Stanhopeinae). *Botanical Journal of the Linnean Society* **176:** 369–383.

Pearse AGE. 1980. *Histochemistry: theoretical and applied*, **Vol. 2**, *4th edn*. Edinburgh: C. Livingstone.

Possobom CCF, **Machado SR. 2017.** Elaiophores: their taxonomic distribution, morphology and functions. *Acta Botanica Brasilica* **31:** 503–524.

Pridgeon AM, **Cribb PJ**, **Chase MW**, **Rasmussen FN, eds. 2009.** *Genera orchidacearum Volume 5; Epidendroideae (Part 2)*. Oxford: Oxford University Press.

Pridgeon AM, **Stern WL. 1983.** Ultrastructure of osmophores in *Restrepia* Kunth (Orchidaceae). *American Journal of Botany* **70:** 1233–1243.

Pridgeon AM, **Stern WL. 1985.** Osmophores of *Scaphosepalum* (Orchidaceae). *Botanical Gazette* **146:** 115–123.

Rasmussen FN. 1985. Orchids. In: Dahlgren RMT, Clifford HT, Yeo PF, eds. *The families of the monocotyledons: structure, evolution and taxonomy*. Berlin: Springer, 247–274.

Reis MG, **Faria AD**, **Alves-dos-Santos I**, **Amaral MCE**, **Marsaioli AJ. 2007.** Byrsonic acid – the clue to floral mimicry involving oil-producing flowers and oil-collecting bees. *Journal of Chemical Ecology* **33:** 1421–1429.

Reis MG, **Faria AD**, **Bittrich V**, **Amaral MCE**, **Marsaioli AJ. 2000.** The chemistry of flower-rewards: *Oncidium* (Orchidaceae). *Journal of the Brazilian Chemical Society* **11:** 600–608.

Reis MG, **Singer RB**, **Gonçalves R**, **Marsaioli AJ. 2006.** The chemical composition of *Phymatidium delicatulum* and *P. tillandsioides* (Orchidaceae) floral oils. *Natural Products Communications* **1:** 757–761.

Remizowa MV, **Rudall PJ**, **Choob VV**, **Sokoloff DD. 2013.** Racemose inflorescences of monocots: structural and morphogenetic interaction at the flower/inflorescence level. *Annals of Botany* **112:** 1553–1566.

Rudolf J. 1993. *Monograph of the genus Gongora Ruiz & Pavón (transl. M. Sommer & C. d'Heureuse)*. Champaign/Königstein: Koeltz Scientific Books.

Sass JE. 1951. *Botanical microtechnique*, *2nd edn*. Ames: Iowa State College Press.

Silva AG. 1990. Osmóforos: retrospectiva dos últimos 20 anos de pesquisa. *Rodriguésia* **42–44:** 7–20.

Silveira K. 2002. *Adaptive radiation of oil-reward compounds among Neotropical orchid species (Oncidiinae)*. Unpublished Master's Thesis, University of Florida.

Simpson BB, **Neff JL. 1981.** Floral rewards: alternatives to pollen and nectar. *Annals of the Missouri Botanical Garden* **68:** 301–322.

Singer RB, **Cocucci AA. 1999.** Pollination mechanisms in four sympatric southern Brazilian Epidendroideae orchids. *Lindleyana* **14:** 47–56.

Spurr AR. 1969. A low-viscosity epoxy resin embedding medium for electron microscopy. *Journal of Ultrastructure Research* **26:** 31–43.

Stern WL, **Curry KJ**, **Pridgeon AM. 1987.** Osmophores of *Stanhopea* (Orchidaceae). *American Journal of Botany* **74:** 1323–1331.

Stpiczyńska M. 1993. Anatomy and ultrastructure of osmophores of *Cymbidium tracyanum* Rolfe (Orchidaceae). *Acta Societatis Botanicorum Poloniae* **62:** 5–9.

Stpiczyńska M. 2001. Osmophores of the fragrant orchid *Gymnadenia conopsea* L. (Orchidaceae). *Acta Societatis Botanicorum Poloniae* **70:** 91–96.

Stpiczyńska M, **Davies KL. 2008.** Elaiophore structure and oil secretion in flowers of *Oncidium trulliferum* Lindl. and *Ornithophora radicans* (Rchb.f.) Garay & Pabst (Oncidiinae: Orchidaceae). *Annals of Botany* **101:** 375–384.

Stpiczyńska M, **Davies KL**, **Gregg A. 2007.** Elaiophore diversity in three contrasting members of Oncidiinae (Orchidaceae). *Botanical Journal of the Linnean Society* **155:** 135–148.

Stpiczyńska M, **Davies KL**, **Pacek-Bieniek A**, **Kamińska M. 2013.** Comparative anatomy of the floral elaiophore in representatives of the newly recircumscribed *Gomesa* and *Oncidium clades* (Orchidaceae: Oncidiinae). *Annals of Botany* **112:** 839–854.

Stpiczyńska M, **Davies KL**, **Zych M**, **Płachno BJ. 2018.** Labellar secretory structures and pollinator food-rewards in representatives of Old World *Bulbophyllum* Thouars. *Flora* **240:** 98–115.

Tölke ED, **Capelli NV**, **Pastori T**, **Alencar AC**, **Cole TCH**, **Demarco D. 2019.** Diversity of floral glands and their secretions in pollinator attraction. In: Merillon JM, Ramawat K, eds. *Co-evolution of secondary metabolites. Reference Series in Phytochemistry*. Cham: Springer.

Van Den Dool H, **Kratz PDA. 1963.** Generalization of the retention index system including linear temperature programmed gas-liquid partition chromatography. *Journal of Chromatography* **11:** 463–471.

Vidal BC. 1970. Dichroism in collagen bundles stained with xylidine Ponceau 2R. *Annales d'histochimie* **15:** 289–296.

Vogel S. 1969. Flowers offering fatty oil instead of nectar. Abstracts, Proceedings of the XI International Botanical Congress, Seattle, 229.

Vogel S. 1974. Ölblumen und ölsammelnde Bienen. *Tropische und subtropische Pflanzenwelt* **7:** 285–547

Vogel S. 1990. *The role of scent glands in pollination*, *1st edn*. Washington: Smithsonian Institution.

Vogel S. 2009. The non-African oil flowers and their bees: a brief survey. SAAB Annual Meeting Abstracts. *South African Journal of Botany* **75:** 389–390.

Weimer AP, **Moré M**, **Benitez-Vieyra S**, **Cocucci AA**, **Raguso RA**, **Sérsic AN. 2009.** A simple floral fragrance and unusual osmophore structure in *Cyclopogon elatus* (Orchidaceae). *Plant Biology* **11:** 508–514.

Whitten WM, **Williams NH. 1992.** Floral fragrances of *Stanhopea* (Orchidaceae). *Lindleyana* **7:** 130–153.

Whitten WM, **Williams NH**, **Chase MW. 2000.** Subtribal and generic relationship of Maxillarieae (Orchidaceae) with emphasis on Stanhopeinae: combined molecular evidence. *American Journal of Botany* **87:** 1842–1856.

Williams NH, **Whitten WM. 1983.** Orchid floral fragrances and male Euglossini bees: methods and advances in the last sesquidecade. *Biological Bulletin* **164:** 355–395.

Withner CL, **Nelson PK**, **Wejks-Nora PJ. 1974.** The anatomy of orchids. In: Withner CL, ed. *The orchids: scientific studies*. New York: John Wiley & Sons, 267–347.

Zimmermann Y, **Roubik DW**, **Eltz T. 2006.** Species-specific attraction to pheromonal analogues in orchid bees. *Behavioral Ecology and Sociobiology* **60:** 833–843.